An effective Decision making model through Fusion Optimization and risk associated with flash flood hazards: A case study Asyut, Egypt

Nabil M. AbdelAziz*, Hassan H. Mohammed, Khalid A. Eldrandaly

Department of Information Systems, Faculty of Computers and Informatics, Zagazig University, Sharqiyah, Egypt.
Emails: nmabedelaziz@fci.zu.edu.eg; helfeky439@gmail.com; Khalid_Eldrandaly@zu.edu.eg

Abstract

One of the most dangerous natural disasters, which causes massive damage all over the world, is flash floods. Therefore, the assessment of flash floods disasters is considered increasingly urgent and important. The widely used techniques for studying and analyzing the causes and impact of natural hazards are multi-criteria techniques. Several researchers used traditional multi-criteria decision-making techniques in the estimation process of flash floods problems as the analytical hierarchy process, decision making trial and evaluation laboratory and analytic network process. The main disadvantage of these traditional models is the incapability of simulating and reflecting uncertain human thoughts. Since neutrosophic logic has a great ability for simulating human's thoughts and increase the flexibility of expert's preferences in real world problems, we applied it in this study. There are different locations in Egypt that are at a serious risk of flooding, especially in Upper Egypt. Asyut has suffered from frequent flash floods, with some flood events that lead to mortality, damages, and economic losses in the last decades. The intensity of floods in Egypt varies from year to year, according to several climatic and hydrological variables. This study focuses on using a Neutrosophic Decision making trial and evaluation laboratory (N-DEMATEL) technique with remotely sensed data and geographical information system (GIS) for producing a flash floods hazard map. The N-DEMATEL technique is applied to determine the weights of various factors that related to flash flooding, including elevation, slope, topographic wetness index, distance from the stream, flow accumulation, aspect, flow direction, soil, land cover, watershed, curvature, drainage density , total population , population density and precipitation. The obtained weight of selected criteria used then to produce the flood hazard map (FHM) using a raster calculator tool in geographic information system.

Keywords: Neutrosophic Set; Multi-Criteria Decision-Making Technique (MCDM); Decision making trial and evaluation laboratory (DEMATEL); Geographic Information System (GIS); Flood Hazard Map.

1. Introduction

As we know, flash floods are considered as one of the most natural disasters which cause massive damage all over the world. In recent decades, flash flood hazards have increased all over the world. Flash flood is caused by severe rainfall on specific area over a short time [1, 2]. Due to climate change, the world is facing increasingly frequent and heavy rainfall [3]. Continuous increases in the concentration of greenhouse gases will cause further global climate change. Climate change is projected to change the floods frequency, magnitude, and severity [4]. Many studies show the effect of climate change on the occurrence of extreme regional phenomena of precipitation and focus on the resulting changes in the volume of precipitation and the occurrence of floods [5]. So, the assessment of flash flood disasters is considered

Doi: https://doi.org/10.54216/FPA.120105
Received: January 17, 2023 Revised: April 25, 2023 Accepted: June 09, 2023

increasingly urgent and important. In recent years, flash flood hazard maps are a very important component to reduce risk of flash floods.

Flash flood risk maps provide residents with information about potential damage and how to prevent probable disasters. These maps are produced in many forms, such as maps for emergency plans, flood tracking, flood hazard reduction and flood information, as well as for many other purposes [6]. Recently, integrating GIS and remote sensing (RS) has been used to produce risk maps. There are many factors that used for producing flash flood susceptibility maps and depends on the effect and importance of each independent factor and varies between different areas, including elevation, slope, topographic wetness index, distance from the stream, flow accumulation, aspect, and flow direction, soil, land cover, watershed, curvature, total population , population density and precipitation [3, 7-9].

There are various locations in Egypt that were subjected to flash floods, which caused human losses and damage to infrastructure [1,2]. Upper Egypt is considered one of the most vulnerable places to floods [10-12] and described in Table1.

Multi-criteria decision-making analysis is a broad term that used to describe several models that facilitate decision making and considering many criteria within a defined system. Several studies have used various multi-criteria decision-making techniques and combined it with remotely sensed data and geographical information system (GIS) for producing a flash flood hazard map. Many authors applied different multi criteria models to assign an optimal criterion weight according to their relative importance Some of the MCDM approaches such as ANP, AHP and TOPSIS have been united with geographical information system and remotely sensed data at flash flood susceptibility assessment [2,9,13-19].

In literature there does not exist any model which combined neutrosophic DEMATEL technique with GIS for analyzing flash floods problems. DEMATEL was first developed by the Science and Human affairs Program of the Battelle Memorial Institute of Geneva [20]. DEMATEL is an effective way to identify the components of the cause chain in a complex system [21]. It deals with evaluating interdependent relationships among factors and finding the critical ones through a visual structural model. Due to its capabilities and advantages, the DEMATEL approach has received a lot of attention in the past decade and many researchers have applied it to solve complex system problems in many fields.

Our study focuses on extending the DEMATEL technique under neutrosophic environment and combining it with remotely sensed data and geographical information system (GIS) for producing a flash flood hazard map.

Table 1: Historical flash floods events in Egypt

Flash flood location	**Date**	**Type of damage**
Giza	1972	180 destroyed houses, 1500 people affected, roads cutoff, and inundation of agricultural areas
Wad El-Arish, Sinai	February 1975	280 destroyed houses, 17 deaths, and thousands became homeless
Sohag, Asyut, and Kom-Ombo in Aswan	May, 1979	200 houses demolished, 3 deaths, 10,000 acres of farmland were flooded
Asyut, Sohag, and Idfu	October, 1979	1576 destroyed houses and 8841 homeless
Kom-Ombo, Aswan	October, 1979	Destruction of nearly three hundred houses
Wadi Watir, Sinai	October, 1987	27 persons were injured, many deaths, highways damages
Wadi Sudr	January, 1988	5 loss of life
Wadi Dahab, Sinai	September, 1994	40% of the highway of Nuweiba City were destroyed
Asyut	November, 1994	Explosion of oil tanks, deaths, various damages, and economic losses in Drunka village
Sinai, Red Sea, and Aswan	January, 2010	Awan: 500 families became homeless, North Sinai: 6 deaths and hundreds were injured, South Sinai: 2 deaths and 16 were injured
Wadi Dahab and Catherine, Sinai	October, 2012	Power were cutoff, and houses were destroyed
South Sinai	January, 2013	2 deaths, 19 injury, Nuweiba roads were partially destroyed and cutoff telecommunication network

Doi: https://doi.org/10.54216/FPA.120105
Received: January 17, 2023 Revised: April 25, 2023 Accepted: June 09, 2023

Qena	January, 2013	Deaths and various damages
Asyut	March, 2014	Dam failure
Sinai and Red Sea	March, 2014	Various damages, destruction events, people deaths, and injuries
Taba, South Sinai	May, 2014	1 death, 7 injures, 70 family were displaced and severe economic losses
Sohag	October, 2016	Partial failure in Sohag Dam
Asyut	November, 2018	Partial failure in Asyut Dam

The structure of this research is planned as follow: Section 2 describes the study area and flash flood influencing factors with details. Section 3 describes some basics of neutrosophic theory. Section 4 describes the proposed method of neutrosophic DEMATEL based GIS. The application of the proposed method is described in section 5. Section 6 describes results and discussions of study area using proposed method. Section 7 summarizes research and conclusions of this study.

2.STUDY AREA AND FLASH FLOOD INFLUENCING FACTORS

Asyut is situated in Upper Egypt and is located between latitudes 26° 45′ to 27° 30′ N and longitudes 30° 30′ to 31° 30′ E as seen in Figure .1 . The study area covers approximately 16,485 km2; the city lies 400 km south of Cairo. Asyut governorate is divided by the river Nile into two sections, western and eastern. Rainfall in the Asyut region is very variable and can happen at high rates and unexpectedly. Susceptibility to floods increases when the rate of rainfall is higher than the ability of the soil to absorb water and is higher than the rate of water evaporation. [3] mentioned in his research that Asyut is an arid area with a desert climate characterized by hot dry summer with a 37.4 °C average monthly temperature during June and a high evaporation rate (average 14.2 mm/day). The total population in Asyut about 4,431,750 million and population density is 330 people per km2. According to the Egyptian Meteorological Authority (EMA) the annual precipitation average in winter reaches 7 mm. Asyut was subjected to heavy rains (96 mm) from the 15th to the 18th of November, 2018 which led to devastating floods [3].

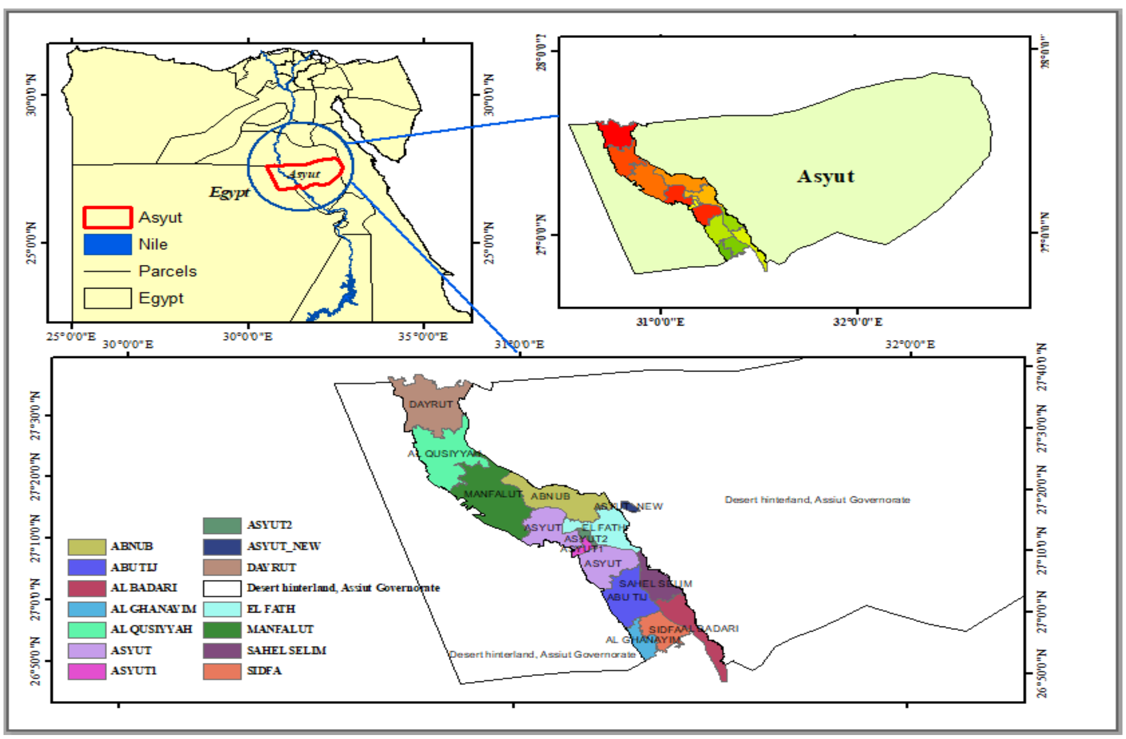

Figure 1: Asyut governorate in Egypt

Doi: https://doi.org/10.54216/FPA.120105
Received: January 17, 2023 Revised: April 25, 2023 Accepted: June 09, 2023

The focus of flood hazard mapping and susceptibility mapping is to determine influencing factors. The determination process of factors, which causes flooding, is mostly based on previous studies and expert opinion in the field. The choice of spatial reference criteria or factors is very important step in decision-making analysis. [22] used the following influencing factors: slope, elevation, distance from stream, and hydrologic units. While [23] assumed factors as follows: slope, cover type, elevation, land use, population density and distance from river and mainstream. Also, [24] used lithology, slope, drainage network, wetness index of topographic, elevation and curvature as influencing factors. As said by [25], geological, hydrogeological, and physio-geographical factors that affect flash floods include slope, soil type, precipitation, catchment area and land use. Also [9] used the following six flood causative factors: digital elevation model (DEM), slope, distance from stream, topographic wetness index (TWI), lithological units, and land use (LULC). Both elevation and slope have the highest values in terms of susceptibility of flooding, while the area of low slopes and low ground elevation are more susceptible to flash floods [24].

From reviewing relevant literature, we selected elevation, slope, topographic wetness index, distance from the stream, flow accumulation, aspect, flow direction, soil, land cover , watershed , curvature , drainage density , total population , population density and precipitation as the main flash flood factors for our study as follows:

2.1 Elevation

Shuttle Radar Topography Mission (SRTM) data with 30 m spatial resolution were acquired from the United State Geological Survey (USGS) http://gdex.cr.usgs.gov/gdex. (SRTM) data are used for extracting the digital elevation model DEM as seen in Figure .2 . The low altitude lands are more prone to flooding, whilst higher land is less prone to flooding. According to [26] areas of lower elevation are more prone to flooding as water is flow into the lowlands more than the highlands. Accordingly, "lower elevation" as a factor increases flood susceptibility.

2.2 Slope

Slope is a measure of the degree of inclination or steepness and is one of the greatest floods influencing factors because it determines the water velocity. Slope is an important in determining risk of flash floods for the reason of its influence on stream water flows and runoff. Areas with gentle slopes are more prone to flooding, as low-lying and sloping areas are the first to be submerged when a flood enters an area. The slope of our study area seen in Figure .3. The low slope degree given the highest rating.

2.3 Topographic Wetness Index (TWI)

TWI is an indicator that determines the ability of the Earth's surface to be saturated with water and could determine overland flow output. TWI pointing to the propensity for flow accumulation determines the influence of topography on hydrological processes, and it is a useful indicator for assessing flood vulnerability [27]. Many researchers have used TWI as an input to develop predictive maps regarding hazard risk of wildfire landslide susceptibility and soil sensitivity. The TWI shown in Figure .4

2.4 Aspect

Aspect is the direction of slope. Aspect has a role on the runoff of surface due to its impact on the other factors like solar radiation, rainfall regime and soil humidity. Aspect starts at the north with 0°, ends at the north with 360° moves and move clockwise. An aspect of 10° is closer than 30° to 360° as it is a circular measure. We must manipulate measures of aspect before using them in data analysis. In our study shown in Figure .5.

2.5 Soil and Land use land cover (LULC)

A soil property, ST describes the relative proportion of different grain sizes of mineral particles in a soil and determines the water infiltration and runoff generation. Soil structure size ranges from fine to medium particle [28]. LULC describes the appearance of the landscape. Soil and LULC data were acquired from food and agriculture organization of the United Nations (FAO). Soil raster and LULC raster are both shown in Figure . 6 and Figure .7.

2.6 Precipitation

Precipitation data during the time period 2011-2020, are downloaded for free from https://crudata.uea.ac.uk/cru/data/hrg/. The analysis of data includes four stages. The images are downloaded in .tif

Doi: https://doi.org/10.54216/FPA.120105
Received: January 17, 2023 Revised: April 25, 2023 Accepted: June 09, 2023

format with GCS projection, then convert the images to Arc-GIS format. The next step is to clip the images to match the study area. The images are converted to points and resampled into 30 m spatial resolution images. The final stage is to estimate the precipitation in no-data areas using IDW (inverse distance weighted) method. The precipitation of our study area seen in Figure .8.

2.7 Curvature

Curvature reflects the morphology of the topography and can affect flooding in each area [29]. Negative, zero and positive curvatures denote concave, flat and convex surfaces [8]. The activity of runoff is associated with the concave surfaces, which are highly susceptible to flooding [30]. The curvature of our study area seen in Figure .9.

2.8 Watershed

Watershed is defined as any surface area from which runoff resulting from rainfall is collected and drained through a common point. It is synonymous with a drainage basin or catchment area. A watershed may be only a few hectares as in small ponds or hundreds of square kilometres as in rivers. The watershed of our study area is seen in Figure .10.

2.9 Total Population and Population Density

Total population and population density are critical parameters for assessment the risk of flash floods. The floods cause huge losses in the lives of residents and property of the local population .[3] mentioned in his paper that "the population of the governorate of Asyut reached 4,431,750 million in 2018 compared to 4,407,335 in 2017 and 4,300,748 in 2016. Population density increased from 260.8 in 2016 to 267.35 in 2017 and 268.8 person/ km2 in 2018". The population data were downloaded for free from Central Agency for Public Mobilization and Statistics, https://www.capmas.gov.eg/ . The population data of our study area seen in Figure .11 and Figure .12.

2.10 Drainage Density

Drainage density is significant in that it plays an important role in surface-runoff processes, influencing the intensity of torrential floods, the concentration, the sediment load and even the water balance in a drainage basin. Drainage density is the total length of streams in a drainage basin divided by the area of the basin. The more extensive the network of streams, the higher the drainage density will be. This measures how fast water drains into streams and rivers. . The drainage density data of our study area is seen in Figure .13.

2.11 Distance from Streams

We used the DEM to extract the drainage network. Several network buffer zones were applied and drainage network classes Figure .14. When the area is close to the drainage network system, it will be more affected by floods.

2.12 Flow Direction and Flow Accumulation

A flow direction raster determines the path of water will flow out of each cell of a filled elevation raster. A flow accumulation raster calculates the number of cells that flow to each cell. Flow direction raster and Flow accumulation raster are both shown in Figure .15 and Figure .16.

Doi: https://doi.org/10.54216/FPA.120105
Received: January 17, 2023 Revised: April 25, 2023 Accepted: June 09, 2023

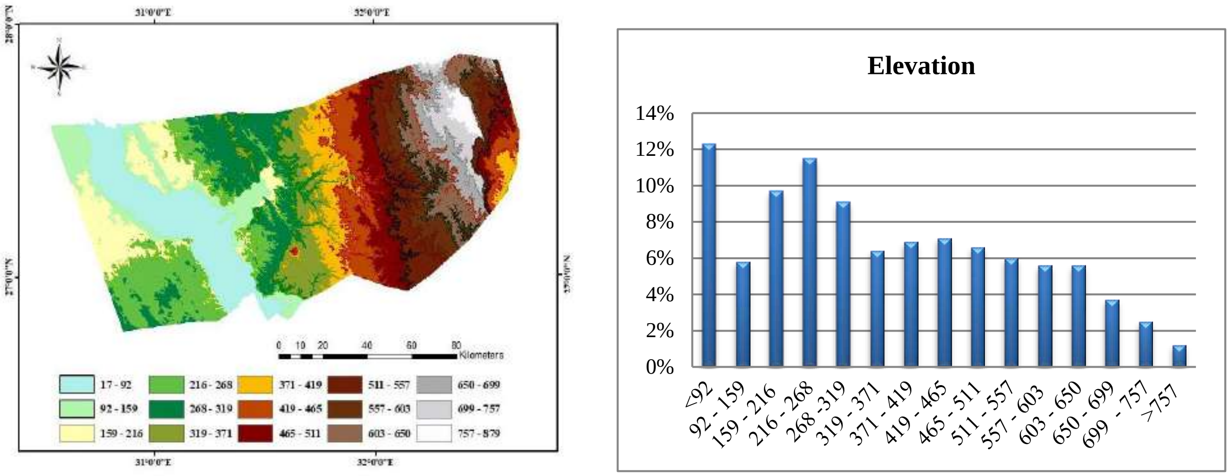

Figure 2: Elevation in Asyut

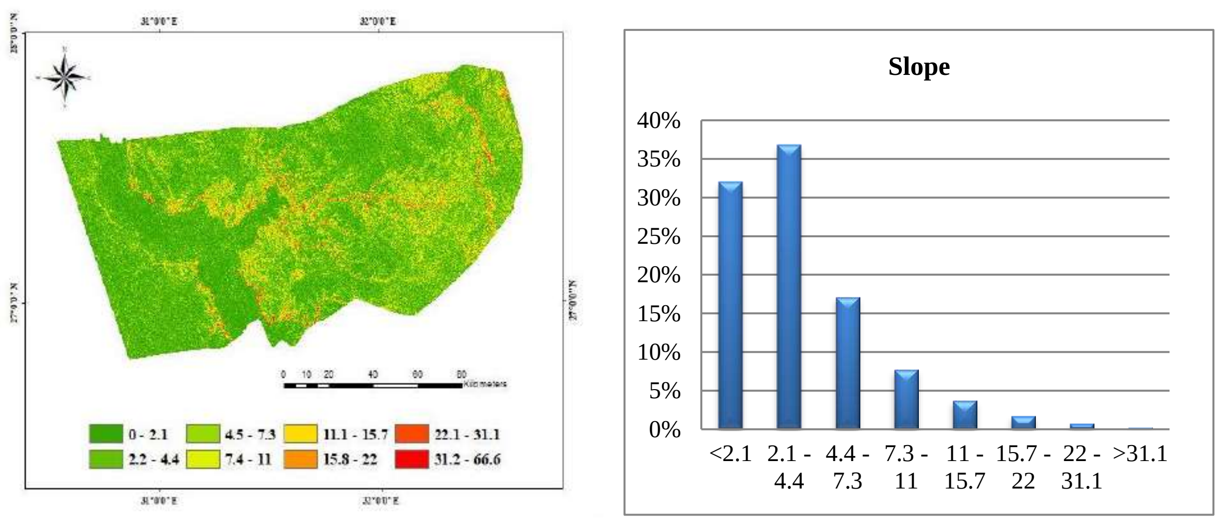

Figure 3: Slope in Asyut

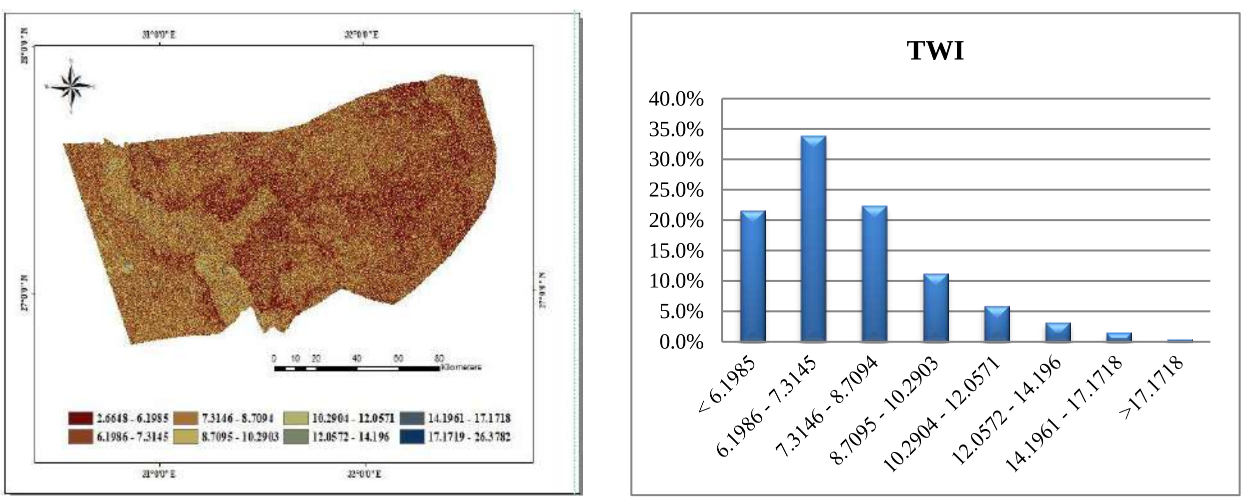

Figure 4: Topographic Wetness Index (TWI) in Asyut

Doi: https://doi.org/10.54216/FPA.120105
Received: January 17, 2023 Revised: April 25, 2023 Accepted: June 09, 2023

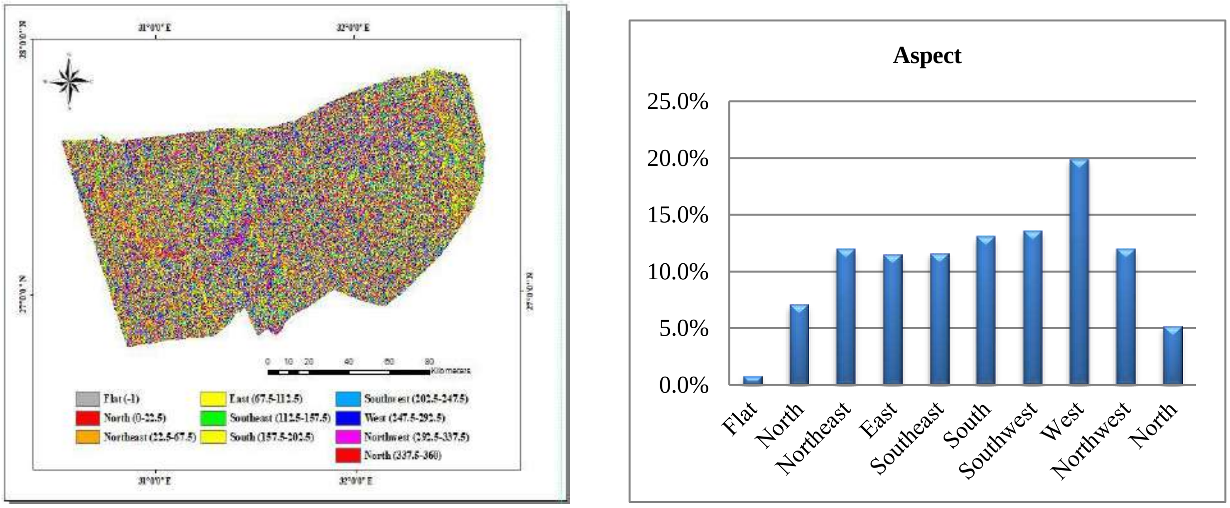

Figure 5: Aspect in Asyut

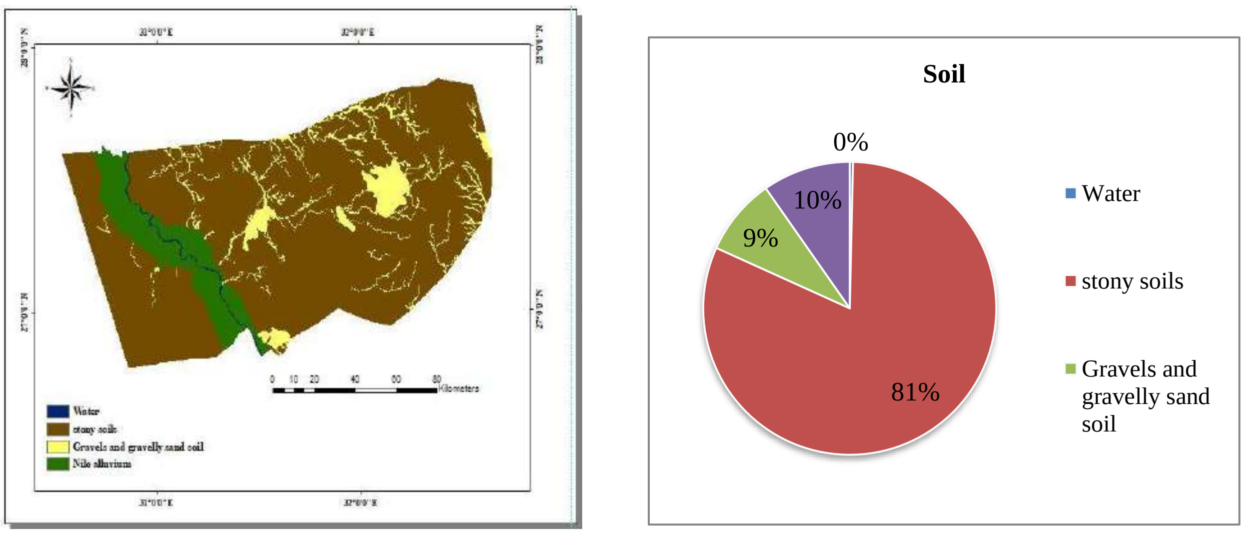

Figure 6: Soil in Asyut

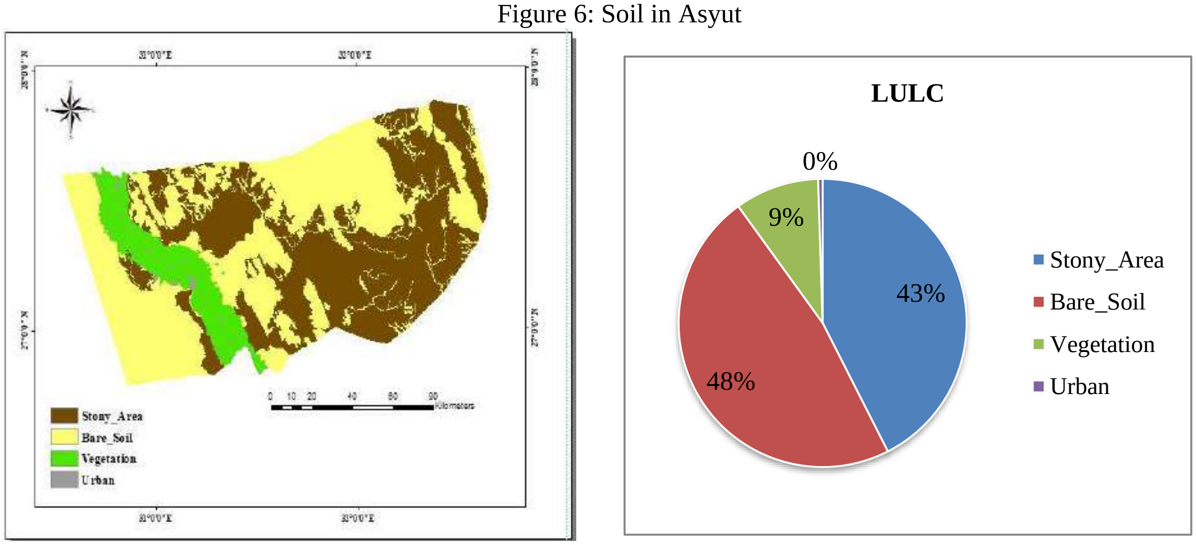

Figure 7: LULC in Asyut

Doi: https://doi.org/10.54216/FPA.120105
Received: January 17, 2023 Revised: April 25, 2023 Accepted: June 09, 2023

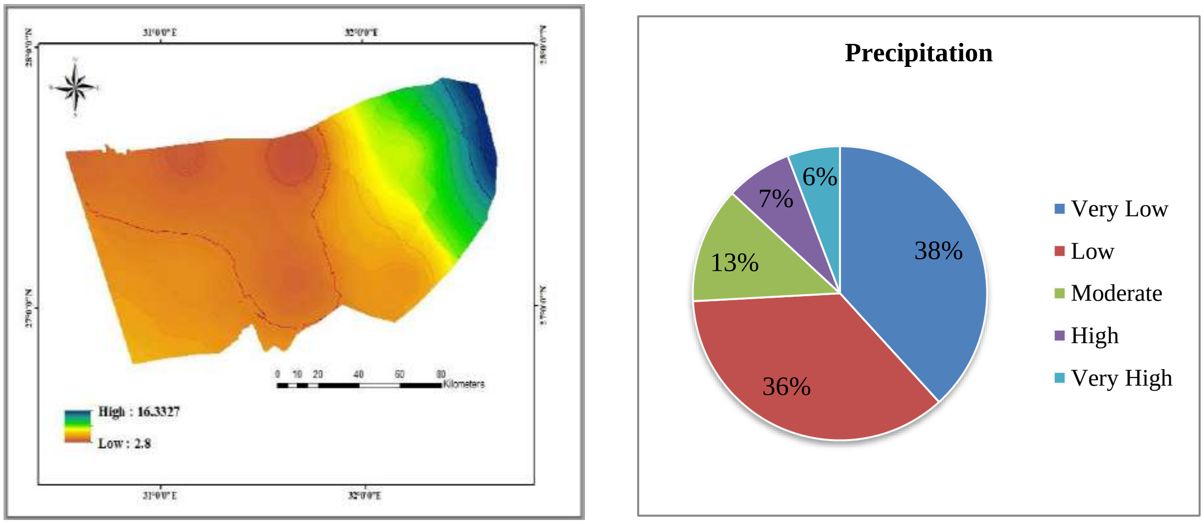

Figure 8: Precipitation in Asyut

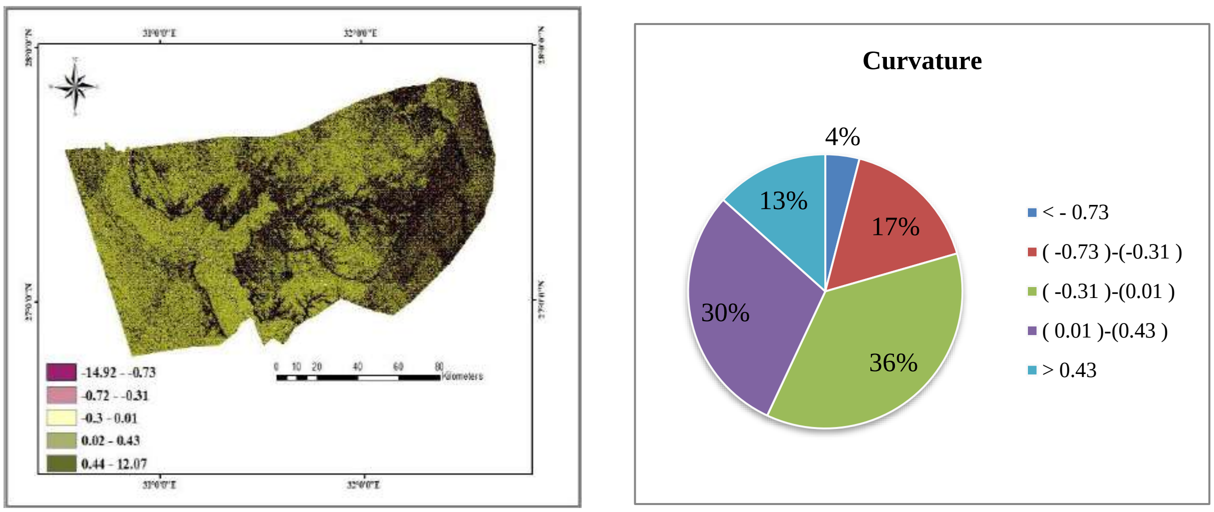

Figure 9: Curvature in Asyut

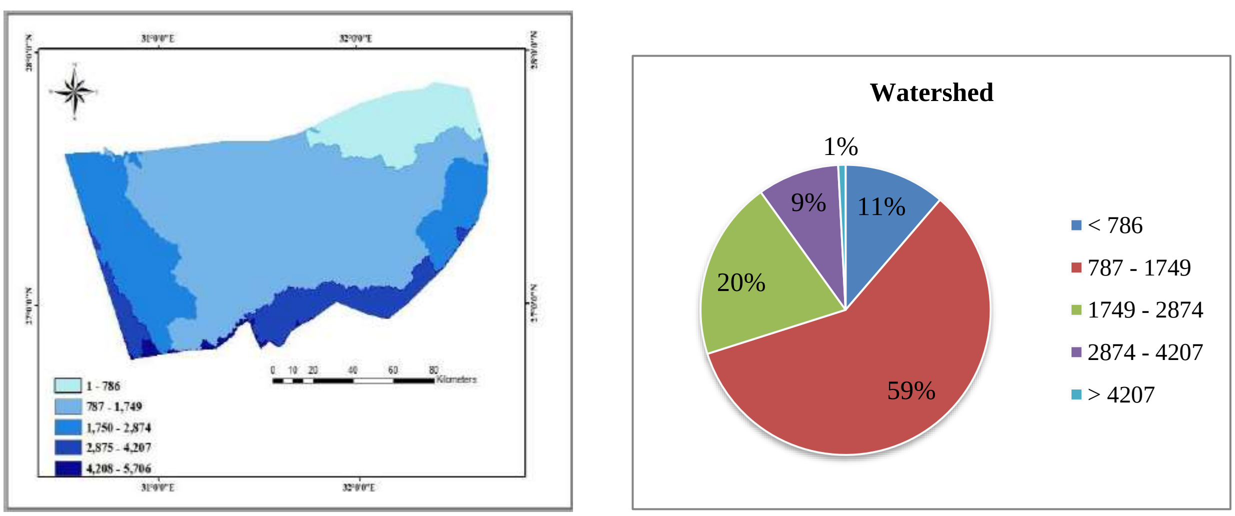

Figure 10: Watershed in Asyut

Doi: https://doi.org/10.54216/FPA.120105
Received: January 17, 2023 Revised: April 25, 2023 Accepted: June 09, 2023

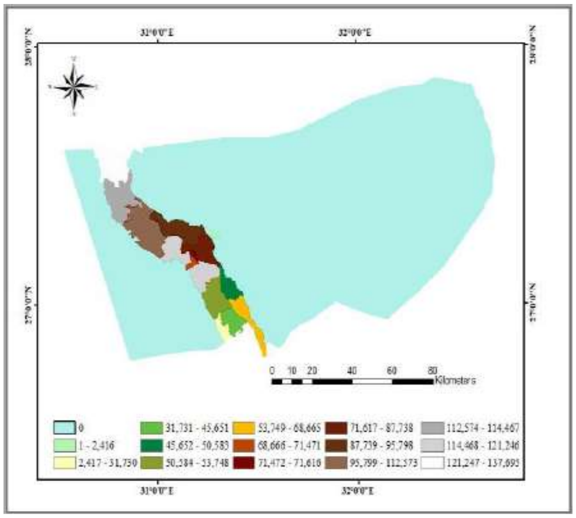

Figure 11: Total population in Asyut

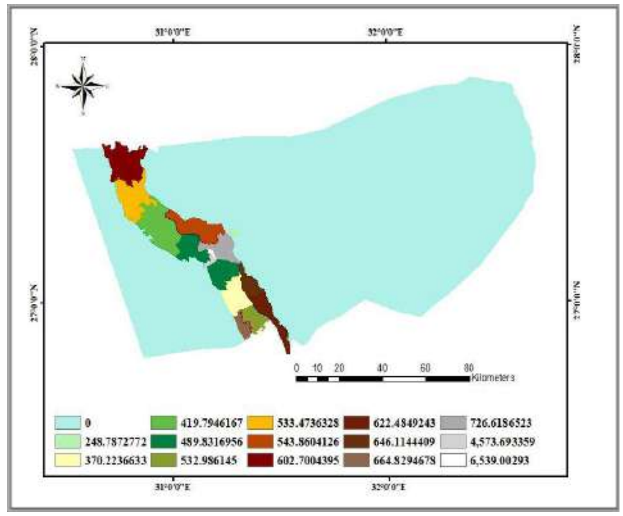

Figure 12: Population Density in Asyut

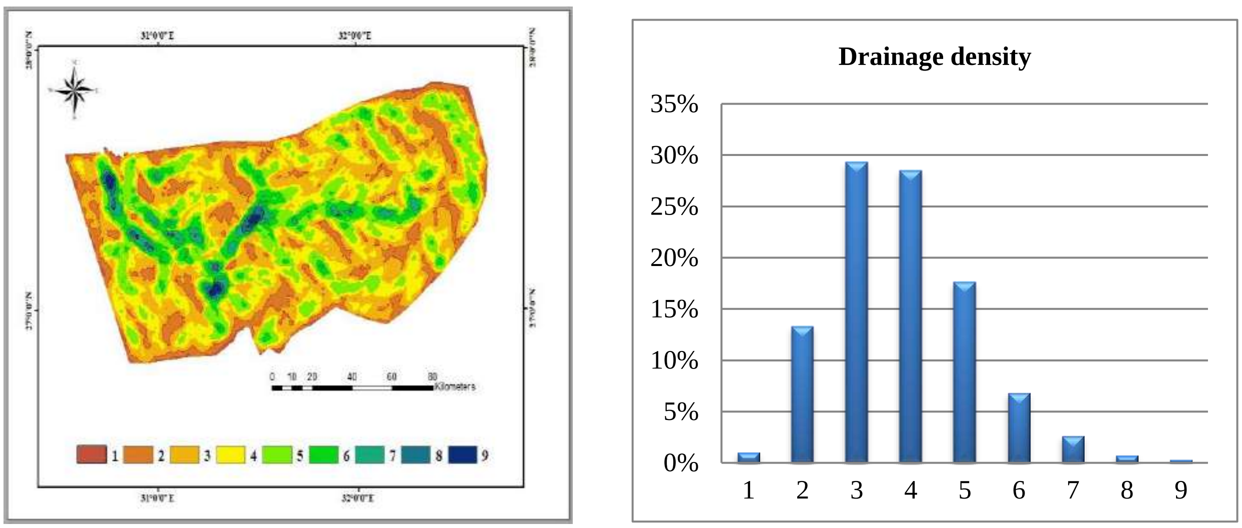

Figure 13: Drainage density in Asyut

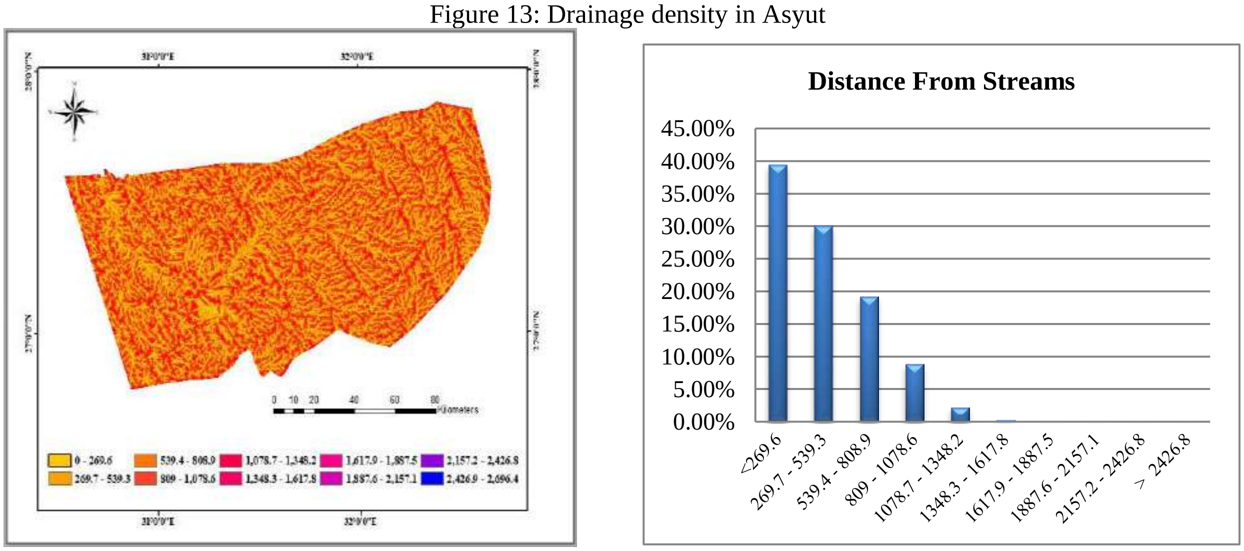

Figure 14: Distance From Streams in Asyut

Doi: https://doi.org/10.54216/FPA.120105
Received: January 17, 2023 Revised: April 25, 2023 Accepted: June 09, 2023

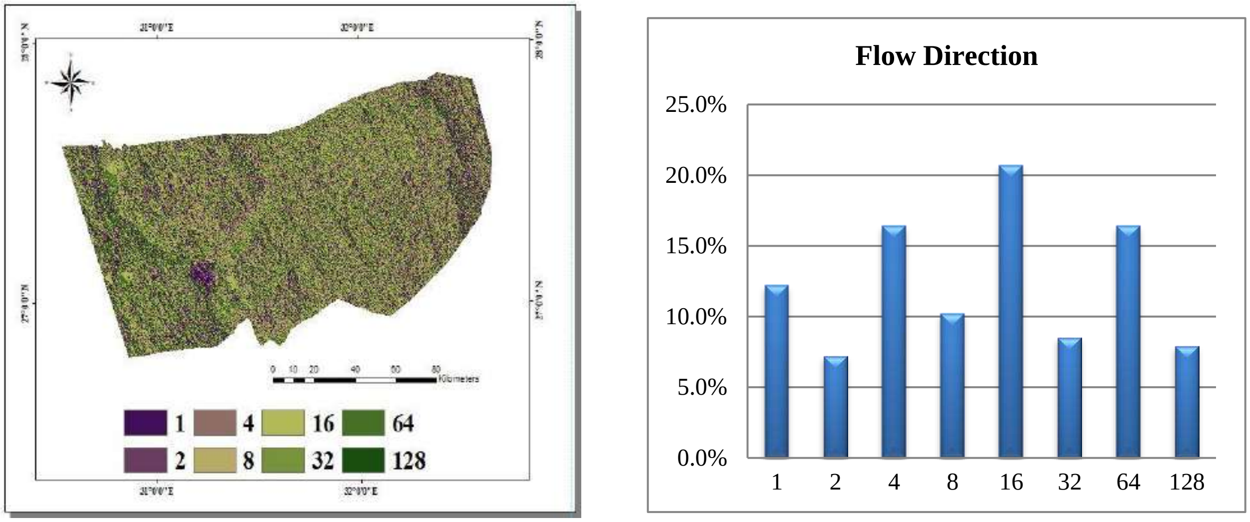

Figure 15: Flow direction in Asyut

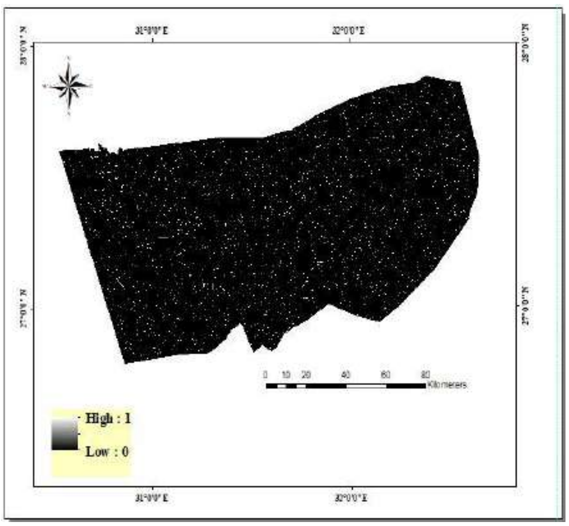

Figure 16: Flow accumulation in Asyut

3. Fusion of NEUTROSOPHIC PRELIMINARIES

The neutrosophic set N has three membership functions which are truth $T_{Ne}(x)$, indeterminacy $I_{Ne}(x)$ and falsity $F_{Ne}(x)$ membership functions, where $T_{Ne}(x){:}X \rightarrow]^{-}0, 1^{+}[$, $I_{Ne}(x){:}X \rightarrow]^{-}0, 1^{+}[$ and $F_{Ne}(x){:}X \rightarrow]^{-}0, 1^{+}[$. This set is free from restriction on the sum of $T_{Ne}(x)$, $I_{Ne}(x)$ and $F_{Ne}(x)$, so $0^{-} \leq \sup T_{Ne}(x) + \sup I_{Ne}(x) + \sup F_{Ne}(x) \leq 3^{+}$ [31]. In [32], An interval valued neutrosophic set INS over X has the following form $A=\{\langle x, T_{Ne}(x), I_{Ne}(x), F_{Ne}(x)\rangle : x \in X\}$ where T_{Ne} is the truth-membership function, I_{Ne} is the indeterminacy-membership function and F_{Ne} is the real falsity-membership function. For each point x in X, we have $T_{Ne}(x) = [T_{Ne}^{L}(x), T_{Ne}^{U}(x)] \subset [0, 1]$, $I_{Ne}(x) = [I_{Ne}^{L}(x), I_{Ne}^{U}(x)] \subset [0, 1]$, $F_{Ne}(x) = [F_{Ne}^{L}(x), F_{Ne}^{U}(x)] \subset [0, 1]$ and $\sup(T_{Ne}^{U}(x)) + \sup(I_{Ne}^{U}(x)) + \sup(F_{Ne}^{U} \leq 3$.

Basic operations of interval valued neutrosophic numbers are as follows:

Let $A = < [T_A^L, T_A^U], [I_A^L, I_A^U], [F_A^L, F_A^U] > \ and\ B = < [T_B^L, T_B^U], [I_B^L, I_B^U], [F_B^L, F_B^U] >$ be two interval valued neutrosophic numbers. Then,

1. $A + B = < [T_A^L + T_B^L - T_A^L * T_B^L,\ T_A^U + T_B^U - T_A^U * T_B^U], [I_A^L * I_B^L, I_A^U * I_B^U], [F_A^L * F_B^L, F_A^U * F_B^U] >.$

Doi: https://doi.org/10.54216/FPA.120105
Received: January 17, 2023 Revised: April 25, 2023 Accepted: June 09, 2023

2. $A * B = < [T_A^L * T_B^L , T_A^U * T_B^U] , [I_A^L + I_B^L - I_A^L * I_B^L, I_A^U + I_B^U - I_A^U * I_B^U] , [F_A^L + F_B^L - F_A^L * F_B^L, F_A^U + F_B^U - F_A^U * F_B^U] >.$
3. $n * A = < [1 - (1 - T_A^L)^n , 1 - (1 - T_A^U)^n] , [(I_A^L)^n, (I_A^U)^n] , [(F_A^L)^n, (F_A^U)^n] >.$
4. $A^n = < [(T_A^L)^n, (T_A^U)^n] , [1 - (1 - I_A^L)^n , 1 - (1 - I_A^U)^n] , [1 - (1 - F_A^L)^n , 1 - (1 - F_A^U)^n] >.$

4. PROPOSED FUSION NEUTROSOPHIC EXTENDED DECISION-MAKING TRIAL AND EVALUATION LABORATORY (N-DEMATEL) TECHNIQUE

There are various methods for evaluating the weights of decision attributes as AHP [33], FARE [34], entropy [35]. DEMATEL was first developed by the Science and Human affairs Program of the Battelle Memorial Institute of Geneva[20]. DEMATEL is an effective way to identify the components of the cause chain in a complex system [21]. The DEMATEL technique has the following advantages: (1) It effectively analyzes the mutual influences (direct and indirect effects) between different factors and understands the complex cause-and-effect relationships in a decision-making problem.(2)It is able to visualize the relationships among the factors via IRM and enable the decision maker to have a clear understanding of the factors that influence each other.(3) DEMATEL can be used not only to determine the order of alternatives, but also to detect important evaluation criteria and measure the weights of the evaluation criteria. [21] mentioned that the possible disadvantages of the DEMATEL technique may be the following: (1) It determines the order of alternatives on the basis of the interrelationships among them; But other criteria were not incorporated into the decision-making problem.(2) The relative weights of experts are not taken into account when aggregating experts' subjective judgments in group assessments.(3) It cannot take into account the level of ambition of the alternatives as in the GRA and VIKOR methods or obtain a partial ranking of the alternatives as in the ELECTRE approach.

The procedure for determination of weights by N- DEMATEL is stated in the steps below:

Step 1: Let decision makers begin to evaluate criteria according to their expected significances using the neutrosophic scale as appears in Table 2

Table 2: The linguistic values and its corresponding neutrosophic values for evaluation process

Linguistic Variable	Corresponding Neutrosophic Values (NV_s)
Absolutely low Significance	<[0.5,0.6],[0.35,0.45] , [0.4,0.5]>
Extremely low Significance	<[0.55,0.65],[0.3,0.4],[0.35,0.45]>
Very Low Significance	<[0.6,0.7],[0.25,0.35],[0.3,0.4]>
Medium Low Significance	<[0.65,0.75],[0.2,0.3],[0.25,0.35]>
Low Significance	<[0.7,0.8],[0.15,0.25],[0.2,0.3]>
Equally significance	<[0.5,0.5],[0.5,0.5],[0.5,0.5]>
High Significance	<[0.75,0.85],[0.1,0.2],[0.15,0.25]>
Medium High Significance	<[0.8,0.9],[0.05,0.1],[0.1,0.2]>
Very High Significance	<[0.9,0.95],[0,0.05],[0.05,0.15]>
Extremely High Significance	<[0.95,1],[0,0],[0,0.1]>
Absolutely High Significance	<[1,1],[0,0],[0,0]>

The previous linguistic variables are used by decision makers to clear their preferences.

Step 2 : Generating the direct relation matrix:

This matrix is obtained from previous step (1), i.e., the integrating of all averaged opinions of experts. An initial direct relation matrix A is a n × n matrix obtained by pairwise comparisons.

Doi: https://doi.org/10.54216/FPA.120105
Received: January 17, 2023 Revised: April 25, 2023 Accepted: June 09, 2023

Step 3 : Normalizing the direct relation matrix.
The normalized direct relation matrix can be obtained using the equation:

$$D = A \times M \text{ , where } M = \frac{1}{MAX_{\ 1 \le i \ge n} \sum_{j=1}^{n} a_{ij}} \qquad (1)$$

Step 4: Attaining the total relation matrix.

This step requires use of the Microsoft Excel software. The total relation matrix is acquired using the formula (2) from the generalized direct relation matrix D. A total relation matrix (T),

in which (I) denotes the identity matrix, is shown as follows:

$$T = D \times (I - D)^{-1} \qquad (2)$$

Step 5: Obtaining the sum of rows and columns.

The sum of rows is denoted by (D), and the sum of columns is denoted by (R). Calculate

R+D and R−D from the total-influence matrix using the formula (3) and (4) .

$$D = \sum_{j=1}^{n} a_{ij} \quad , i = 1,2,3, \dots \dots \dots , n \qquad (3)$$

$$R = \sum_{i=1}^{n} a_{ij} \quad , j = 1,2,3, \dots \dots \dots , n \qquad (4)$$

Step 6 : Drawing cause and effect diagram

The causal diagram is obtained by the horizontal axes is presented by (D+R) and the vertical axes (D−R) which is a degree of relation and it depicts the steps of proposed model in Figure 17.

Step 7 : calculate the weights of criteria .
The priority weight of each criterion can be calculated as follows:

$$W_i = \frac{D_i + R_i}{\sum_{i=1}^{n}(D_i + R_i)} \quad , i = 1,2,3, \dots \dots \dots , n \qquad (5)$$

Doi: https://doi.org/10.54216/FPA.120105
Received: January 17, 2023 Revised: April 25, 2023 Accepted: June 09, 2023

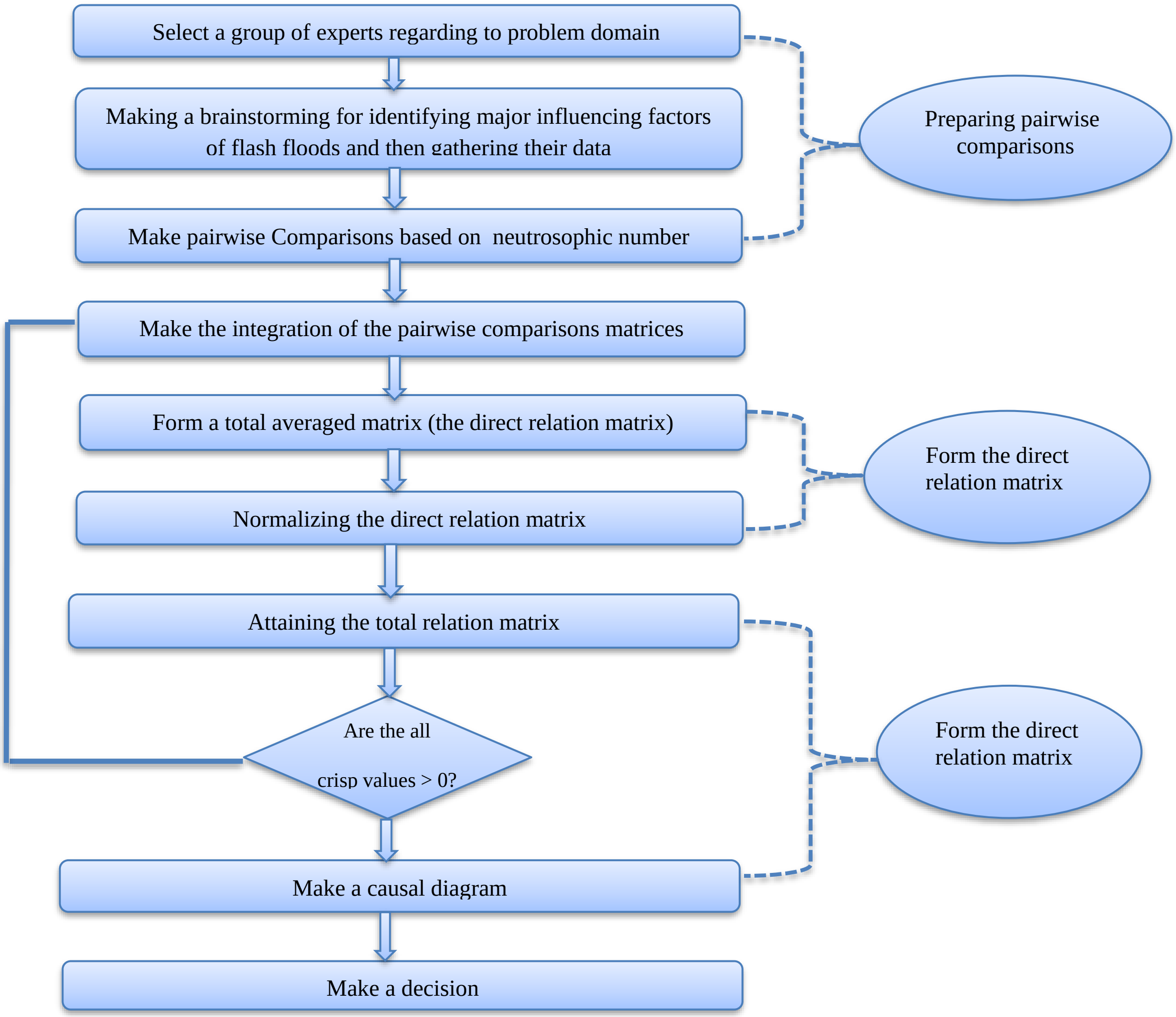

Figure 17: Schematic diagram of DEMATEL in neutrosophic environment

5. Fusion of NEUTROSOPHIC N-DEMATEL ANALYSIS FOR WEIGHTING FLOOD INFLUENCING FACTORS

In our study, we are the first to propose an extended single interval valued neutrosophic DEMATEL technique based on GIS for analyzing flash floods. The N-DEMATEL used to obtain weights of flood influencing factors and combined into the GIS - environment to create flood susceptibility maps. The integration of GIS-environment with neutrosophic DEMATEL analysis provides more flexibility for to assess the causative agents of flooding. The general framework of proposed model for analyzing flash floods appears in Figure .18.

Doi: https://doi.org/10.54216/FPA.120105
Received: January 17, 2023 Revised: April 25, 2023 Accepted: June 09, 2023

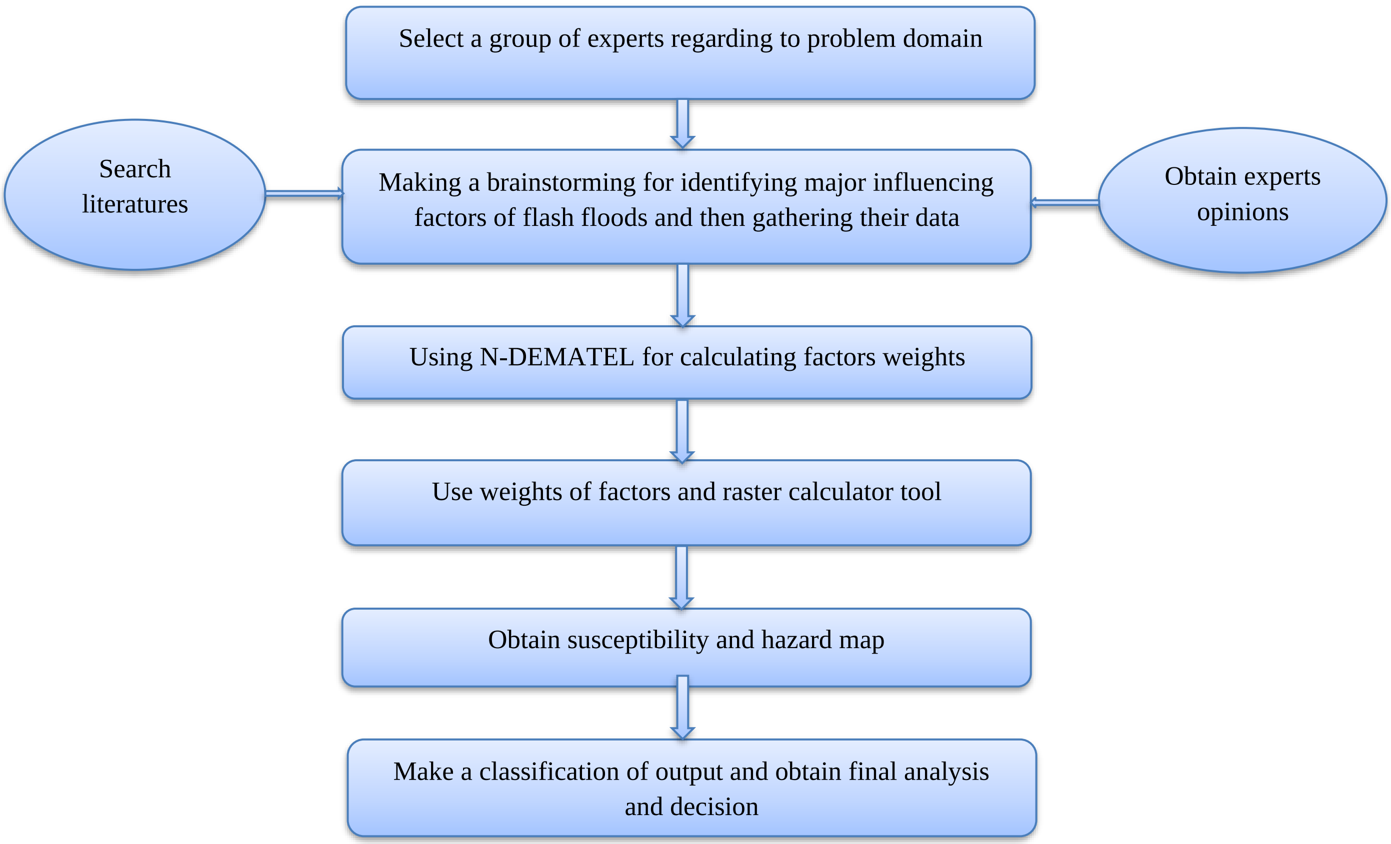

Figure 18: Study methodology

Since in our study area we discuss various factors related to flash flooding as elevation, slope, topographic wetness index, distance from the stream, flow accumulation, aspect, flow direction , soil , land cover , watershed , curvature , drainage density , total population , population density and precipitation. So, let us now use proposed algorithm for calculating its weights and then make analysis of flash floods as follows:

Step 1: Previous studies were used to evaluate criteria using neutrosophic linguistic variables which presented in Table 2 [3 , 7-9] and obtained data which presented in Table3.

Table 3 :The neutrosophic values for evaluating criteria : C1(Population Density) , C2(Total Population) , C3(Precipitation) , C4(Distance From Stream) , C5(DEM) , C6(DrainageDensity) , C7(Soil) , C8(LULC) , C9(Slope) , C10(Flow Direction) , C11(Flow Accumulation) , C12(TWI) , C13(Curvature) , C14(Aspect) , C15(Watershed).

	C1	**C2**	**C3**	**C4**	**C5**	**C6**	**C7**	**C8**	**C9**	**C10**	**C11**	**C12**	**C13**	**C14**	**C15**
C1	ES	HS	HS	MHS	MHS	MHS	EHS	VHS	MHS	EHS	EHS	EHS	EHS	AHS	AHS
C2	LS	ES	HS	MHS	MHS	MHS	EHS	VHS	MHS	EHS	EHS	EHS	EHS	AHS	AHS
C3	LS	LS	ES	VHS	MHS	HS	MHS	MHS	HS	EHS	VHS	EHS	EHS	AHS	AHS
C4	MLS	MLS	VLS	ES	HS	MHS	HS	VHS	MHS	EHS	EHS	EHS	EHS	AHS	AHS
C5	MLS	MLS	MLS	LS	ES	MHS	HS	MHS	MHS	VHS	VHS	EHS	VHS	VHS	AHS
C6	MLS	MLS	LS	MLS	MLS	ES	MHS	VHS	MHS	EHS	EHS	EHS	EHS	AHS	AHS

Doi: https://doi.org/10.54216/FPA.120105
Received: January 17, 2023 Revised: April 25, 2023 Accepted: June 09, 2023

C7	ELS	ELS	MLS	LS	LS	MLS	ES	HS	HS	MHS	HS	VHS	EHS	VHS	VHS
C8	VLS	VLS	MLS	VLS	MLS	VLS	LS	ES	HS	MHS	MHS	VHS	EHS	VHS	VHS
C9	MLS	MLS	LS	MLS	MLS	MLS	LS	LS	ES	HS	HS	MHS	MHS	VHS	VHS
C10	ELS	ELS	ELS	ELS	VLS	ELS	MLS	MLS	LS	ES	HS	MHS	MHS	VHS	VHS
C11	ELS	ELS	VLS	ELS	VLS	ELS	LS	MLS	LS	LS	ES	MHS	MHS	VHS	VHS
C12	ELS	ELS	ELS	ELS	ELS	ELS	VLS	VLS	MLS	MLS	MLS	ES	HS	MHS	MHS
C13	ELS	ELS	ELS	ELS	VLS	ELS	ELS	ELS	MLS	MLS	MLS	LS	ES	MHS	MHS
C14	ALS	ALS	ALS	ALS	VLS	ALS	VLS	VLS	VLS	VLS	VLS	MLS	MLS	ES	VHS
C15	ALS	ALS	ALS	ALS	ALS	ALS	VLS	VLS	VLS	VLS	VLS	MLS	MLS	VLS	ES

Then, the single-valued interval neutrosophic fuzzy direct-relation decision matrix is formed as A={⟨x,$T_{Ne}(x)$, $I_{Ne}(x)$, $F_{Ne}(x)$⟩:x∈X} where T_{Ne} is the truth-membership function, I_{Ne} is the indeterminacy-membership function and F_{Ne} is the real falsity-membership function as presented in Table 4.

Step2 : Normalize the direct-relation decision matrix A to $D = < [T_D^L, T_D^U], [I_D^L, I_D^U], [F_D^L, F_D^U] >$, $T_D^L = \frac{T_A^L}{K}$, $T_D^U = \frac{T_A^U}{K}$, $K = max\left\{\max_{1\le i\ge n}\sum_{j=1}^{n} T_{A\,ij}^{L}, \max_{1\le j\ge n}\sum_{i=1}^{n} T_{A\,ij}^{U}\right\}$ · $I_D^L = \frac{I_A^L}{K}$, $I_D^U = \frac{I_A^U}{K}$, $K = max\left\{\max_{1\le i\ge n}\sum_{j=1}^{n} I_{A\,ij}^{L}, \max_{1\le j\ge n}\sum_{i=1}^{n} I_{A\,ij}^{U}\right\}$ · $F_D^L = \frac{F_A^L}{K}$, $F_D^U = \frac{F_A^U}{K}$, $K = max\left\{\max_{1\le i\ge n}\sum_{j=1}^{n} F_{A\,ij}^{L}, \max_{1\le j\ge n}\sum_{i=1}^{n} F_{A\,ij}^{L}\right\}$ see (Appendix A).

Step3 : Calculate the total-relation matrix $\widetilde{D}$, which can be calculated by using the six crisp Normalize direct-relation decision matrix D where $\widetilde{D} = < [T_{\widetilde{D}}^L, T_{\widetilde{D}}^U], [I_{\widetilde{D}}^L, I_{\widetilde{D}}^U], [F_{\widetilde{D}}^L, F_{\widetilde{D}}^U] >$,

$T_{\widetilde{D}}^L = T_D^L \times (I - T_D^L)^{-1}$, $T_{\widetilde{D}}^U = T_D^U \times (I - T_D^U)^{-1}$, $I_{\widetilde{D}}^L = I_D^L \times (I - I_D^L)^{-1}$, $I_{\widetilde{D}}^U = I_D^I \times (I - I_D^U)^{-1}$, $F_{\widetilde{D}}^L = F_D^L \times (I - F_D^L)^{-1}$, $F_{\widetilde{D}}^U = F_D^U \times (I - F_D^U)^{-1}$ as presented in Table 5.

Table 4: single-valued interval neutrosophic fuzzy direct-relation decision matrix

	C1	**C2**	**C3**
C1	<[0.5,0.5],[0.5,0.5],[0.5,0.5]>	<[0.75,0.85],[0.1,0.2],[0.15,0.25]>	<[0.75,0.85],[0.1,0.2],[0.15,0.25]>
C2	<[0.7,0.8],[0.15,0.25],[0.2,0.3]>	<[0.5,0.5],[0.5,0.5],[0.5,0.5]>	<[0.75,0.85],[0.1,0.2],[0.15,0.25]>
C3	<[0.7,0.8],[0.15,0.25],[0.2,0.3]>	<[0.7,0.8],[0.15,0.25],[0.2,0.3]>	<[0.5,0.5],[0.5,0.5],[0.5,0.5]>
C4	<[0.65,0.75],[0.2,0.3],[0.25,0.35]>	<[0.65,0.75],[0.2,0.3],[0.25,0.35]>	<[0.6,0.7],[0.25,0.35],[0.3,0.4]>
C5	<[0.65,0.75],[0.2,0.3],[0.25,0.35]>	<[0.65,0.75],[0.2,0.3],[0.25,0.35]>	<[0.65,0.75],[0.2,0.3],[0.25,0.35]>
C6	<[0.65,0.75],[0.2,0.3],[0.25,0.35]>	<[0.65,0.75],[0.2,0.3],[0.25,0.35]>	<[0.7,0.8],[0.15,0.25],[0.2,0.3]>

Doi: https://doi.org/10.54216/FPA.120105
Received: January 17, 2023 Revised: April 25, 2023 Accepted: June 09, 2023

C7	<[0.55,0.65],[0.3,0.4],[0.35,0.45]>	<[0.55,0.65],[0.3,0.4],[0.35,0.45]>	<[0.65,0.75],[0.2,0.3],[0.25,0.35]>
C8	<[0.6,0.7],[0.25,0.35],[0.3,0.4]>	<[0.6,0.7],[0.25,0.35],[0.3,0.4]>	<[0.65,0.75],[0.2,0.3],[0.25,0.35]>
C9	<[0.65,0.75],[0.2,0.3],[0.25,0.35]>	<[0.65,0.75],[0.2,0.3],[0.25,0.35]>	<[0.7,0.8],[0.15,0.25],[0.2,0.3]>
C10	<[0.55,0.65],[0.3,0.4],[0.35,0.45]>	<[0.55,0.65],[0.3,0.4],[0.35,0.45]>	<[0.55,0.65],[0.3,0.4],[0.35,0.45]>
C11	<[0.55,0.65],[0.3,0.4],[0.35,0.45]>	<[0.55,0.65],[0.3,0.4],[0.35,0.45]>	<[0.6,0.7],[0.25,0.35],[0.3,0.4]>
C12	<[0.55,0.65],[0.3,0.4],[0.35,0.45]>	<[0.55,0.65],[0.3,0.4],[0.35,0.45]>	<[0.55,0.65],[0.3,0.4],[0.35,0.45]>
C13	<[0.55,0.65],[0.3,0.4],[0.35,0.45]>	<[0.55,0.65],[0.3,0.4],[0.35,0.45]>	<[0.55,0.65],[0.3,0.4],[0.35,0.45]>
C14	<[0.5,0.6],[0.35,0.45],[0.4,0.5]>	<[0.5,0.6],[0.35,0.45],[0.4,0.5]>	<[0.5,0.6],[0.35,0.45],[0.4,0.5]>
C15	<[0.5,0.6],[0.35,0.45],[0.4,0.5]>	<[0.5,0.6],[0.35,0.45],[0.4,0.5]>	<[0.5,0.6],[0.35,0.45],[0.4,0.5]>

Table 4 :(continued)

	C4	**C5**	**C6**
C1	<[0.8,0.9],[0.05,0.1],[0.1,0.2]>	<[0.8,0.9],[0.05,0.1],[0.1,0.2]>	<[0.8,0.9],[0.05,0.1],[0.1,0.2]>
C2	<[0.8,0.9],[0.05,0.1],[0.1,0.2]>	<[0.8,0.9],[0.05,0.1],[0.1,0.2]>	<[0.8,0.9],[0.05,0.1],[0.1,0.2]>
C3	<[0.9,0.95],[0,0.05],[0.05,0.15]>	<[0.8,0.9],[0.05,0.1],[0.1,0.2]>	<[0.75,0.85],[0.1,0.2],[0.15,0.25]>
C4	<[0.5,0.5],[0.5,0.5],[0.5,0.5]>	<[0.75,0.85],[0.1,0.2],[0.1,50.25]>	<[0.8,0.9],[0.05,0.1],[0.1,0.2]>
C5	<[0.7,0.8],[0.15,0.25],[0.2,0.3]>	<[0.5,0.5],[0.5,0.5],[0.5,0.5]>	<[0.8,0.9],[0.05,0.1],[0.1,0.2]>
C6	<[0.65,0.75],[0.2,0.3],[0.25,0.35]>	<[0.65,0.75],[0.2,0.3],[0.25,0.35]>	<[0.5,0.5],[0.5,0.5],[0.5,0.5]>
C7	<[0.7,0.8],[0.15,0.25],[0.2,0.3]>	<[0.7,0.8],[0.15,0.25],[0.2,0.3]>	<[0.65,0.75],[0.2,0.3],[0.25,0.35]>
C8	<[0.6,0.7],[0.25,0.35],[0.3,0.4]>	<[0.65,0.75],[0.2,0.3],[0.2,50.35]>	<[0.6,0.7],[0.25,0.35],[0.3,0.4]>
C9	<[0.65,0.75],[0.2,0.3],[0.25,0.35]>	<[0.65,0.75],[0.2,0.3],[0.25, 0.35]>	<[0.65,0.75],[0.2,0.3],[0.25,0.35]>
C10	<[0.55,0.65],[0.3,0.4],[0.35,0.45]>	<[0.6,0.7],[0.25,0.35],[0.3,0.4]>	<[0.55,0.65],[0.3,0.4],[0.35,0.45]>
C11	<[0.55,0.65],[0.3,0.4],[0.35,0.45]>	<[0.6,0.7],[0.25,0.35],[0.3,0.4]>	<[0.55,0.65],[0.3,0.4],[0.35,0.45]>
C12	<[0.55,0.65],[0.3,0.4],[0.35,0.45]>	<[0.55,0.65],[0.3,0.4],[0.35,0.45]>	<[0.55,0.65],[0.3,0.4],[0.35,0.45]>
C13	<[0.55,0.65],[0.3,0.4],[0.35,0.45]>	<[0.6,0.7],[0.25,0.35],[0.3,0.4]>	<[0.55,0.65],[0.3,0.4],[0.35,0.45]>
C14	<[0.5,0.6],[0.35,0.45],[0.4,0.5]>	<[0.6,0.7],[0.25,0.35],[0.3,0.4]>	<[0.5,0.6],[0.35,0.45],[0.4,0.5]>
C15	<[0.5,0.6],[0.35,0.45],[0.4,0.5]>	<[0.5,0.6],[0.35,0.45],[0.4,0.5]>	<[0.5,0.6],[0.35,0.45],[0.4,0.5]>

Table 4 :(continued)

	C7	**C8**	**C9**

Doi: https://doi.org/10.54216/FPA.120105
Received: January 17, 2023 Revised: April 25, 2023 Accepted: June 09, 2023

C1	<[0.95,1],[0,0],[0,0.1]>	<[0.9,0.95],[0,0.05],[0.05,0.15]>	<[0.8,0.9],[0.05,0.1],[0.1,0.2]>
C2	<[0.95,1],[0,0],[0,0.1]>	<[0.9,0.95],[0,0.05],[0.05,0.15]>	<[0.8,0.9],[0.05,0.1],[0.1,0.2]>
C3	<[0.8,0.9],[0.05,0.1],[0.1,0.2]>	<[0.8,0.9],[0.05,0.1],[0.1,0.2]>	<[0.75,0.85],[0.1,0.2],[0.15,0.25]>
C4	<[0.75,0.85],[0.1,0.2],[0.15,0.25]>	<[0.9,0.95],[0,0.05],[0.05,0.15]>	<[0.8,0.9],[0.05,0.1],[0.1,0.2]>
C5	<[0.75,0.85],[0.1,0.2],[0.15,0.25]>	<[0.8,0.9],[0.05,0.1],[0.1,0.2]>	<[0.8,0.9],[0.05,0.1],[0.1,0.2]>
C6	<[0.8,0.9],[0.05,0.1],[0.1,0.2]>	<[0.9,0.95],[0,0.05],[0.05,0.15]>	<[0.8,0.9],[0.05,0.1],[0.1,0.2]>
C7	<[0.5,0.5],[0.5,0.5],[0.5,0.5]>	<[0.75,0.85],[0.1,0.2],[0.15,0.25]>	<[0.75,0.85],[0.1,0.2],[0.15,0.25]>
C8	<[0.7,0.8],[0.15,0.25],[0.2,0.3]>	<[0.5,0.5],[0.5,0.5],[0.5,0.5]>	<[0.75,0.85],[0.1,0.2],[0.15,0.25]>
C9	<[0.7,0.8],[0.15,0.25],[0.2,0.3]>	<[0.7,0.8],[0.15,0.25],[0.2,0.3]>	<[0.5,0.5],[0.5,0.5],[0.5,0.5]>
C10	<[0.65,0.75],[0.2,0.3],[0.25,0.35]>	<[0.65,0.75],[0.2,0.3],[0.25,0.35]>	<[0.7,0.8],[0.15,0.25],[0.2,0.3]>
C11	<[0.7,0.8],[0.15,0.25],[0.2,0.3]>	<[0.65,0.75],[0.2,0.3],[0.25,0.35]>	<[0.7,0.8],[0.15,0.25],[0.2,0.3]>
C12	<[0.6,0.7],[0.25,0.35],[0.3,0.4]>	<[0.6,0.7],[0.25,0.35],[0.3,0.4]>	<[0.65,0.75],[0.2,0.3],[0.25,0.35]>
C13	<[0.55,0.65],[0.3,0.4],[0.35,0.45]>	<[0.55,0.65],[0.3,0.4],[0.35,0.45]>	<[0.65,0.75],[0.2,0.3],[0.25,0.35]>
C14	<[0.6,0.7],[0.25,0.35],[0.3,0.4]>	<[0.6,0.7],[0.25,0.35],[0.3,0.4]>	<[0.6,0.7],[0.25,0.35],[0.3,0.4]>
C15	<[0.6,0.7],[0.25,0.35],[0.3,0.4]>	<[0.6,0.7],[0.25,0.35],[0.3,0.4]>	<[0.6,0.7],[0.25,0.35],[0.3,0.4]>

Table 4 :(continued)

	C10	**C11**	**C12**
C1	<[0.95,1],[0,0],[0,0.1]>	<[0.95,1],[0,0],[0,0.1]>	<[0.95,1],[0,0],[0,0.1]>
C2	<[0.95,1],[0,0],[0,0.1]>	<[0.95,1],[0,0],[0,0.1]>	<[0.95,1],[0,0],[0,0.1]>
C3	<[0.95,1],[0,0],[0,0.1]>	<[0.9,0.95],[0,0.05],[0.05,0.15]>	<[0.95,1],[0,0],[0,0.1]>
C4	<[0.95,1],[0,0],[0,0.1]>	<[0.95,1],[0,0],[0,0.1]>	<[0.95,1],[0,0],[0,0.1]>
C5	<[0.9,0.95],[0,0.05],[0.05,0.15]>	<[0.9,0.95],[0,0.05],[0.05,0.15]>	<[0.95,1],[0,0],[0,0.1]>
C6	<[0.95,1],[0,0],[0,0.1]>	<[0.95,1],[0,0],[0,0.1]>	<[0.95,1],[0,0],[0,0.1]>
C7	<[0.8,0.9],[0.05,0.1],[0.1,0.2]>	<[0.75,0.85],[0.1,0.2],[0.15,0.25]>	<[0.9,0.95],[0,0.05],[0.05,0.15]>
C8	<[0.8,0.9],[0.05,0.1],[0.1,0.2]>	<[0.8,0.9],[0.05,0.1],[0.1,0.2]>	<[0.9,0.95],[0,0.05],[0.05,0.15]>
C9	<[0.75,0.85],[0.1,0.2],[0.15,0.25]>	<[0.75,0.85],[0.1,0.2],[0.15,0.25]>	<[0.8,0.9],[0.05,0.1],[0.1,0.2]>
C10	<[0.5,0.5],[0.5,0.5],[0.5,0.5]>	<[0.75,0.85],[0.1,0.2],[0.15,0.25]>	<[0.8,0.9],[0.05,0.1],[0.1,0.2]>
C11	<[0.7,0.8],[0.15,0.25],[0.2,0.3]>	<[0.5,0.5],[0.5,0.5],[0.5,0.5]>	<[0.8,0.9],[0.05,0.1],[0.1,0.2]>
C12	<[0.65,0.75],[0.2,0.3],[0.25,0.35]>	<[0.65,0.75],[0.2,0.3],[0.25,0.35]>	<[0.5,0.5],[0.5,0.5],[0.5,0.5]>
C13	<[0.65,0.75],[0.2,0.3],[0.25,0.35]>	<[0.65,0.75],[0.2,0.3],[0.25,0.35]>	<[0.7,0.8],[0.15,0.25],[0.2,0.3]>

Doi: https://doi.org/10.54216/FPA.120105
Received: January 17, 2023 Revised: April 25, 2023 Accepted: June 09, 2023

C14	<[0.6,0.7],[0.25,0.35],[0.3,0.4]>	<[0.6,0.7],[0.25,0.35],[0.3,0.4]>	<[0.65,0.75],[0.2,0.3],[0.25,0.35]>
C15	<[0.6,0.7],[0.25,0.35],[0.3,0.4]>	<[0.6,0.7],[0.25,0.35],[0.3,0.4]>	<[0.65,0.75],[0.2,0.3],[0.25,0.35]>

Table 4 :(continued)

	C13	**C14**	**C15**
C1	<[0.95,1],[0,0],[0,0.1]>	<[1,1],[0,0],[0,0]>	<[1,1],[0,0],[0,0]>
C2	<[0.95,1],[0,0],[0,0.1]>	<[1,1],[0,0],[0,0]>	<[1,1],[0,0],[0,0]>
C3	<[0.95,1],[0,0],[0,0.1]>	<[1,1],[0,0],[0,0]>	<[1,1],[0,0],[0,0]>
C4	<[0.95,1],[0,0],[0,0.1]>	<[1,1],[0,0],[0,0]>	<[1,1],[0,0],[0,0]>
C5	<[0.9,0.95],[0,0.05],[0.05,0.15]>	<[0.9,0.95],[0,0.05],[0.05,0.15]>	<[1,1],[0,0],[0,0]>
C6	<[0.95,1],[0,0],[0,0.1]>	<[1,1],[0,0],[0,0]>	<[1,1],[0,0],[0,0]>
C7	<[0.95,1],[0,0],[0,0.1]>	<[0.9,0.95],[0,0.05],[0.05,0.15]>	<[0.9,0.95],[0,0.05],[0.05,0.15]>
C8	<[0.95,1],[0,0],[0,0.1]>	<[0.9,0.95],[0,0.05],[0.05,0.15]>	<[0.9,0.95],[0,0.05],[0.05,0.15]>
C9	<[0.8,0.9],[0.05,0.1],[0.1,0.2]>	<[0.9,0.95],[0,0.05],[0.05,0.15]>	<[0.9,0.95],[0,0.05],[0.05,0.15]>
C10	<[0.8,0.9],[0.05,0.1],[0.1,0.2]>	<[0.9,0.95],[0,0.05],[0.05,0.15]>	<[0.9,0.95],[0,0.05],[0.05,0.15]>
C11	<[0.8,0.9],[0.05,0.1],[0.1,0.2]>	<[0.9,0.95],[0,0.05],[0.05,0.15]>	<[0.9,0.95],[0,0.05],[0.05,0.15]>
C12	<[0.75,0.85],[0.1,0.2],[0.15,0.25]>	<[0.8,0.9],[0.05,0.1],[0.1,0.2]>	<[0.8,0.9],[0.05,0.1],[0.1,0.2]>
C13	<[0.5,0.5],[0.5,0.5],[0.5,0.5]>	<[0.8,0.9],[0.05,0.1],[0.1,0.2]>	<[0.8,0.9],[0.05,0.1],[0.1,0.2]>
C14	<[0.65,0.75],[0.2,0.3],[0.25,0.35]>	<[0.5,0.5],[0.5,0.5],[0.5,0.5]>	<[0.9,0.95],[0,0.05],[0.05,0.15]>
C15	<[0.65,0.75],[0.2,0.3],[0.25,0.35]>	<[0.6,0.7],[0.25,0.35],[0.3,0.4]>	<[0.5,0.5],[0.5,0.5],[0.5,0.5]>

Table 5 : The total-relation matrix T

	C1	**C2**	**C3**
C1	<[0.20,0.35],[0.10,0.11],[0.08,0.11]>	<[0.21,0.38],[0.02,0.05],[0.03,0.07]>	<[0.22,0.39],[0.02,0.05],[0.03,0.07]>
C2	<[0.21,0.37],[0.03,0.06],[0.04,0.08]>	<[0.20,0.35],[0.10,0.11],[0.08,0.11]>	<[0.22,0.39],[0.02,0.05],[0.03,0.07]>
C3	<[0.20,0.36],[0.03,0.07],[0.04,0.09]>	<[0.21,0.37],[0.03,0.07],[0.04,0.09]>	<[0.20,0.35],[0.10,0.11],[0.08,0.12]>
C4	<[0.20,0.35],[0.05,0.08],[0.05,0.10]>	<[0.20,0.36],[0.05,0.08],[0.05,0.10]>	<[0.20,0.36],[0.05,0.09],[0.06,0.10]>
C5	<[0.19,0.35],[0.05,0.09],[0.05,0.11]>	<[0.19,0.35],[0.05,0.09],[0.05,0.11]>	<[0.20,0.36],[0.05,0.09],[0.05,0.10]>
C6	<[0.20,0.35],[0.05,0.08],[0.05,0.10]>	<[0.20,0.35],[0.05,0.08],[0.05,0.10]>	<[0.21,0.37],[0.04,0.07],[0.04,0.09]>
C7	<[0.18,0.33],[0.07,0.12],[0.08,0.14]>	<[0.18,0.33],[0.07,0.12],[0.08,0.14]>	<[0.19,0.34],[0.05,0.10],[0.06,0.12]>
C8	<[0.18,0.33],[0.06,0.12],[0.07,0.13]>	<[0.18,0.33],[0.06,0.11],[0.07,0.13]>	<[0.19,0.34],[0.05,0.10],[0.06,0.12]>
C9	<[0.18,0.33],[0.06,0.11],[0.06,0.13]>	<[0.18,0.33],[0.06,0.11],[0.06,0.13]>	<[0.19,0.34],[0.04,0.10],[0.05,0.12]>

Doi: https://doi.org/10.54216/FPA.120105
Received: January 17, 2023 Revised: April 25, 2023 Accepted: June 09, 2023

C10	<[0.16,0.30],[0.08,0.14],[0.08,0.16]>	<[0.16,0.31],[0.08,0.14],[0.08,0.15]>	<[0.17,0.31],[0.08,0.14],[0.08,0.15]>
C11	<[0.16,0.31],[0.08,0.14],[0.08,0.15]>	<[0.16,0.31],[0.08,0.14],[0.08,0.15]>	<[0.17,0.32],[0.07,0.13],[0.07,0.14]>
C12	<[0.16,0.29],[0.09,0.16],[0.09,0.17]>	<[0.16,0.29],[0.09,0.16],[0.09,0.17]>	<[0.16,0.30],[0.09,0.15],[0.09,0.16]>
C13	<[0.15,0.29],[0.09,0.16],[0.09,0.17]>	<[0.15,0.29],[0.09,0.16],[0.09,0.17]>	<[0.16,0.30],[0.09,0.16],[0.09,0.16]>
C14	<[0.15,0.28],[0.11,0.18],[0.11,0.19]>	<[0.15,0.28],[0.11,0.18],[0.10,0.19]>	<[0.15,0.28],[0.10,0.18],[0.10,0.18]>
C15	<[0.14,0.27],[0.11,0.20],[0.11,0.20]>	<[0.14,0.27],[0.11,0.19],[0.11,0.19]>	<[0.14,0.28],[0.11,0.19],[0.11,0.19]>

Table 5 :(continued)

	C4	**C5**	**C6**
C1	<[0.23,0.40],[0.01,0.03],[0.02,0.06]>	<[0.23,0.41],[0.01,0.03],[0.02,0.06]>	<[0.23,0.40],[0.01,0.03],[0.02,0.06]>
C2	<[0.23,0.390.01,0.03],[0.02,0.06]>	<[0.23,0.40],[0.01,0.03],[0.02,0.06]>	<[0.23,0.40],[0.01,0.03],[0.02,0.06]>
C3	<[0.23,0.39],[0.00,0.03],[0.01,0.06]>	<[0.23,0.40],[0.01,0.03],[0.02,0.07]>	<[0.22,0.39],[0.02,0.05],[0.03,0.07]>
C4	<[0.20,0.35],[0.10,0.11],[0.08,0.11]>	<[0.22,0.39],[0.02,0.05],[0.03,0.08]>	<[0.22,0.38],[0.01,0.03],[0.02,0.07]>
C5	<[0.21,0.37],[0.03,0.07],[0.04,0.09]>	<[0.20,0.36],[0.10,0.11],[0.09,0.12]>	<[0.21,0.38],[0.01,0.04],[0.03,0.08]>
C6	<[0.21,0.37],[0.04,0.07],[0.05,0.09]>	<[0.21,0.38],[0.04,0.07],[0.05,0.09]>	<[0.20,0.35],[0.10,0.11],[0.08,0.11]>
C7	<[0.19,0.35],[0.04,0.08],[0.05,0.11]>	<[0.20,0.36],[0.04,0.08],[0.05,0.10]>	<[0.19,0.35],[0.05,0.09],[0.05,0.11]>
C8	<[0.19,0.34],[0.06,0.10],[0.06,0.12]>	<[0.19,0.35],[0.05,0.09],[0.05,0.11]>	<[0.19,0.34],[0.06,0.10],[0.06,0.12]>
C9	<[0.19,0.34],[0.05,0.10],[0.06,0.12]>	<[0.19,0.35],[0.05,0.10],[0.06,0.12]>	<[0.19,0.35],[0.05,0.10],[0.06,0.12]>
C10	<[0.17,0.32],[0.07,0.13],[0.08,0.14]>	<[0.18,0.33],[0.06,0.11],[0.07,0.13]>	<[0.17,0.32],[0.07,0.12],[0.08,0.14]>
C11	<[0.17,0.32],[0.07,0.13],[0.08,0.14]>	<[0.18,0.33],[0.06,0.11],[0.07,0.13]>	<[0.17,0.32],[0.07,0.12],[0.08,0.14]>
C12	<[0.16,0.30],[0.08,0.14],[0.08,0.16]>	<[0.17,0.31],[0.08,0.14],[0.08,0.15]>	<[0.16,0.31],[0.08,0.14],[0.08,0.15]>
C13	<[0.16,0.30],[0.08,0.14],[0.09,0.16]>	<[0.17,0.31],[0.07,0.13],[0.08,0.15]>	<[0.16,0.30],[0.08,0.14],[0.08,0.16]>
C14	<[0.15,0.29],[0.10,0.16],[0.10,0.17]>	<[0.16,0.30],[0.08,0.14],[0.08,0.15]>	<[0.15,0.29],[0.10,0.16],[0.10,0.17]>
C15	<[0.15,0.28],[0.10,0.17],[0.10,0.18]>	<[0.15,0.29],[0.10,0.17],[0.10,0.18]>	<[0.15,0.28],[0.10,0.17],[0.10,0.18]>

Table 5 :(continued)

	C7	**C8**	**C9**
C1	<[0.26,0.44],[0.00,0.01],[0.00,0.04]>	<[0.26,0.43],[0.00,0.01],[0.01,0.05]>	<[0.25,0.43],[0.01,0.03],[0.02,0.06]>

Doi: https://doi.org/10.54216/FPA.120105
Received: January 17, 2023 Revised: April 25, 2023 Accepted: June 09, 2023

C2	<[0.26,0.43],[0.00,0.01],[0.00,0.04]>	<[0.26,0.43],[0.00,0.01],[0.01,0.05]>	<[0.25,0.43],[0.01,0.03],[0.02,0.06]>
C3	<[0.24,0.42],[0.01,0.03],[0.02,0.06]>	<[0.24,0.42],[0.01,0.03],[0.02,0.06]>	<[0.24,0.42],[0.02,0.05],[0.03,0.07]>
C4	<[0.23,0.41],[0.02,0.05],[0.03,0.07]>	<[0.25,0.42],[0.00,0.02],[0.01,0.05]>	<[0.24,0.42],[0.01,0.03],[0.02,0.06]>
C5	<[0.23,0.40],[0.02,0.05],[0.03,0.08]>	<[0.23,0.41],[0.01,0.03],[0.02,0.07]>	<[0.23,0.41],[0.01,0.04],[0.02,0.07]>
C6	<[0.23,0.41],[0.01,0.03],[0.02,0.06]>	<[0.24,0.41],[0.00,0.02],[0.01,0.05]>	<[0.24,0.41],[0.01,0.03],[0.02,0.06]>
C7	<[0.20,0.36],[0.10,0.12],[0.09,0.12]>	<[0.22,0.39],[0.02,0.06],[0.03,0.08]>	<[0.22,0.39],[0.03,0.06],[0.03,0.09]>
C8	<[0.21,0.38],[0.03,0.07],[0.04,0.09]>	<[0.20,0.36],[0.10,0.11],[0.09,0.12]>	<[0.22,0.39],[0.03,0.06],[0.04,0.09]>
C9	<[0.21,0.38],[0.04,0.08],[0.04,0.10]>	<[0.21,0.38],[0.03,0.07],[0.04,0.10]>	<[0.20,0.36],[0.10,0.12],[0.09,0.13]>
C10	<[0.19,0.35],[0.05,0.09],[0.05,0.11]>	<[0.20,0.35],[0.05,0.09],[0.05,0.11]>	<[0.20,0.36],[0.04,0.08],[0.05,0.10]>
C11	<[0.20,0.36],[0.04,0.08],[0.05,0.10]>	<[0.20,0.36],[0.05,0.09],[0.05,0.11]>	<[0.20,0.36],[0.04,0.08],[0.05,0.10]>
C12	<[0.18,0.33],[0.06,0.11],[0.07,0.13]>	<[0.18,0.34],[0.06,0.11],[0.07,0.13]>	<[0.19,0.34],[0.05,0.10],[0.06,0.12]>
C13	<[0.18,0.33],[0.07,0.12],[0.08,0.14]>	<[0.18,0.33],[0.07,0.12],[0.07,0.14]>	<[0.18,0.34],[0.05,0.10],[0.06,0.12]>
C14	<[0.17,0.32],[0.07,0.12],[0.07,0.14]>	<[0.18,0.32],[0.06,0.12],[0.07,0.14]>	<[0.17,0.32],[0.07,0.12],[0.07,0.14]>
C15	<[0.17,0.31],[0.07,0.13],[0.07,0.14]>	<[0.17,0.31],[0.07,0.12],[0.07,0.14]>	<[0.17,0.32],[0.07,0.13],[0.07,0.14]>

Table 5 :(continued)

	C10	**C11**	**C12**
C1	<[0.28,0.46],[0.00,0.00],[0.00,0.03]>	<[0.28,0.46],[0.00,0.00],[0.00,0.03]>	<[0.29,0.48],[0.00,0.00],[0.00,0.03]>
C2	<[0.28,0.46],[0.00,0.00],[0.00,0.03]>	<[0.27,0.46],[0.00,0.00],[0.00,0.03]>	<[0.29,0.48],[0.00,0.00],[0.00,0.03]>
C3	<[0.27,0.45],[0.00,0.00],[0.00,0.04]>	<[0.27,0.45],[0.00,0.01],[0.01,0.04]>	<[0.28,0.47],[0.00,0.00],[0.00,0.03]>
C4	<[0.26,0.44],[0.00,0.00],[0.00,0.04]>	<[0.26,0.44],[0.00,0.01],[0.00,0.04]>	<[0.28,0.46],[0.00,0.00],[0.00,0.03]>
C5	<[0.26,0.43],[0.00,0.02],[0.01,0.05]>	<[0.26,0.43],[0.00,0.02],[0.01,0.05]>	<[0.27,0.46],[0.00,0.00],[0.00,0.04]>
C6	<[0.26,0.44],[0.00,0.00],[0.00,0.04]>	<[0.26,0.44],[0.00,0.00],[0.00,0.04]>	<[0.28,0.46],[0.00,0.00],[0.00,0.03]>
C7	<[0.23,0.41],[0.01,0.03],[0.02,0.07]>	<[0.23,0.41],[0.02,0.05],[0.03,0.07]>	<[0.25,0.43],[0.00,0.02],[0.01,0.05]>
C8	<[0.23,0.41],[0.01,0.03],[0.02,0.07]>	<[0.23,0.41],[0.01,0.03],[0.02,0.07]>	<[0.25,0.43],[0.00,0.01],[0.01,0.05]>
C9	<[0.23,0.40],[0.02,0.05],[0.03,0.08]>	<[0.23,0.40],[0.02,0.05],[0.03,0.08]>	<[0.24,0.42],[0.01,0.03],[0.02,0.06]>
C10	<[0.20,0.36],[0.10,0.11],[0.08,0.12]>	<[0.21,0.38],[0.02,0.06],[0.03,0.08]>	<[0.23,0.40],[0.01,0.03],[0.02,0.07]>
C11	<[0.21,0.38],[0.03,0.06],[0.04,0.09]>	<[0.20,0.36],[0.10,0.11],[0.08,0.12]>	<[0.23,0.40],[0.01,0.03],[0.02,0.07]>

Doi: https://doi.org/10.54216/FPA.120105
Received: January 17, 2023 Revised: April 25, 2023 Accepted: June 09, 2023

C12	<[0.20,0.36],[0.05,0.08],[0.05,0.10]>	<[0.20,0.36],[0.05,0.08],[0.05,0.11]>	<[0.20,0.36],[0.10,0.10],[0.08,0.12]>
C13	<[0.20,0.36],[0.05,0.08],[0.05,0.11]>	<[0.20,0.35],[0.05,0.08],[0.05,0.11]>	<[0.21,0.37],[0.03,0.06],[0.04,0.09]>
C14	<[0.19,0.34],[0.06,0.10],[0.06,0.12]>	<[0.19,0.34],[0.06,0.10],[0.06,0.12]>	<[0.20,0.36],[0.04,0.07],[0.05,0.10]>
C15	<[0.18,0.33],[0.06,0.10],[0.06,0.12]>	<[0.18,0.33],[0.06,0.10],[0.06,0.12]>	<[0.19,0.35],[0.05,0.08],[0.05,0.10]>

Table 5 :(continued)

	C13	C14	C15
C1	<[0.29,0.48],[0.00,0.00],[0.00,0.03]>	<[0.31,0.49],[0.00,0.00],[0.00,0.01]>	<[0.31,0.50],[0.00,0.00],[0.00,0.01]>
C2	<[0.29,0.48],[0.00,0.00],[0.00,0.03]>	<[0.30,0.49],[0.00,0.00],[0.00,0.01]>	<[0.31,0.50],[0.00,0.00],[0.00,0.01]>
C3	<[0.28,0.47],[0.00,0.00],[0.00,0.03]>	<[0.30,0.48],[0.00,0.00],[0.00,0.01]>	<[0.31,0.49],[0.00,0.00],[0.00,0.01]>
C4	<[0.28,0.47],[0.00,0.00],[0.00,0.03]>	<[0.29,0.47],[0.00,0.00],[0.00,0.01]>	<[0.30,0.48],[0.00,0.00],[0.00,0.01]>
C5	<[0.27,0.45],[0.00,0.01],[0.01,0.04]>	<[0.28,0.46],[0.00,0.01],[0.01,0.04]>	<[0.29,0.47],[0.00,0.00],[0.00,0.01]>
C6	<[0.28,0.46],[0.00,0.00],[0.00,0.03]>	<[0.29,0.47],[0.00,0.00],[0.00,0.01]>	<[0.30,0.48],[0.00,0.00],[0.00,0.01]>
C7	<[0.26,0.44],[0.00,0.01],[0.00,0.04]>	<[0.26,0.44],[0.00,0.01],[0.01,0.04]>	<[0.27,0.45],[0.00,0.01],[0.01,0.04]>
C8	<[0.26,0.43],[0.00,0.01],[0.00,0.04]>	<[0.26,0.44],[0.00,0.01],[0.01,0.04]>	<[0.27,0.44],[0.00,0.01],[0.01,0.04]>
C9	<[0.24,0.43],[0.01,0.03],[0.02,0.06]>	<[0.26,0.44],[0.00,0.02],[0.01,0.04]>	<[0.27,0.44],[0.00,0.01],[0.01,0.04]>
C10	<[0.23,0.40],[0.01,0.03],[0.02,0.07]>	<[0.25,0.41],[0.00,0.02],[0.01,0.04]>	<[0.25,0.42],[0.00,0.01],[0.01,0.04]>
C11	<[0.23,0.40],[0.01,0.03],[0.02,0.07]>	<[0.25,0.41],[0.00,0.02],[0.01,0.04]>	<[0.25,0.42],[0.00,0.01],[0.01,0.04]>
C12	<[0.22,0.38],[0.02,0.05],[0.03,0.08]>	<[0.23,0.39],[0.01,0.03],[0.02,0.06]>	<[0.23,0.40],[0.01,0.03],[0.02,0.05]>
C13	<[0.20,0.35],[0.10,0.10],[0.08,0.12]>	<[0.23,0.39],[0.01,0.03],[0.02,0.06]>	<[0.23,0.40],[0.01,0.03],[0.02,0.05]>
C14	<[0.20,0.36],[0.04,0.07],[0.05,0.10]>	<[0.20,0.35],[0.09,0.10],[0.08,0.10]>	<[0.23,0.39],[0.00,0.02],[0.01,0.05]>
C15	<[0.19,0.35],[0.05,0.08],[0.05,0.10]>	<[0.20,0.35],[0.05,0.08],[0.05,0.09]>	<[0.20,0.34],[0.09,0.10],[0.08,0.10]>

Step 4 : Obtaining the sum of rows and columns using the predefined formula (3) and (4) .
The sum of rows is denoted by (D), and the sum of columns is denoted by (R).

Step 5 : Calculate the weights of attributes by using the formula (6) , as presented in Table 7 and Figure .19.

$$W_i = \frac{\sqrt{((S(D_i+R_i))^2 + (S(D_i-R_i))^2}}{\sum_{i=1}^{n}\sqrt{((S(D_i+R_i))^2 + (S(D_i-R_i))^2}} \quad i = 1,2,3, \dots \dots \dots n \qquad (6)$$

Table 6: The relative weights for each criterion using N-DEMATEL technique

Criteria	Weights

Doi: https://doi.org/10.54216/FPA.120105
Received: January 17, 2023 Revised: April 25, 2023 Accepted: June 09, 2023

C15	**0.06728011**
C1	**0.067037378**
C2	**0.066978636**
C14	**0.06695252**
C13	**0.066892234**
C12	**0.066809228**
C3	**0.066754041**
C4	**0.066496641**
C5	**0.066489133**
C11	**0.066444645**
C10	**0.066417786**
C6	**0.066384715**
C8	**0.06637841**
C9	**0.066355817**
C7	**0.066328707**

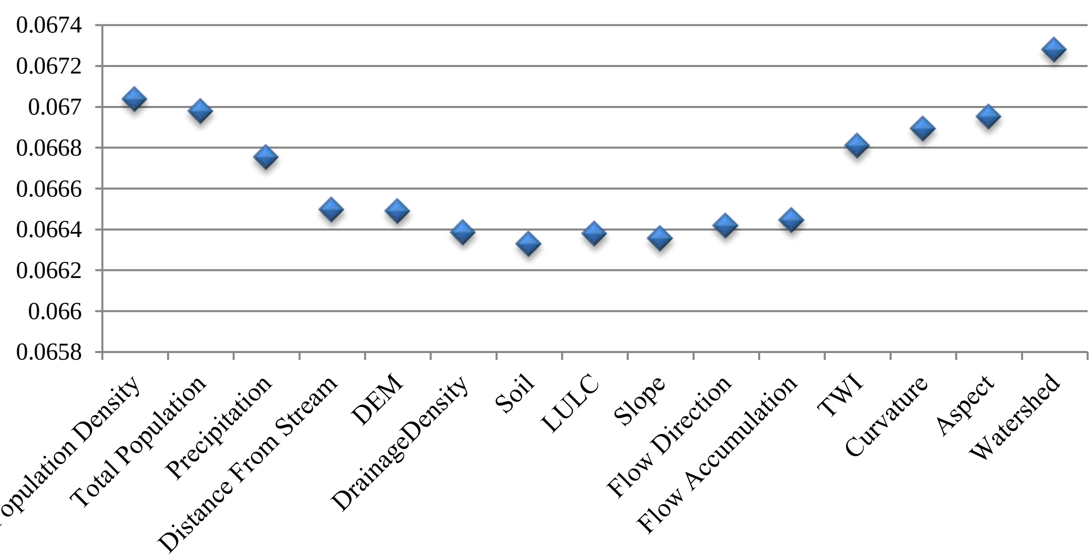

Figure 19: Weights of flash floods controlling factors

6. RESULTS AND DISCUSSION

The applications of a multi-criteria decision-making analysis in our study area were used for evaluating the relative weights of flood controlling factor. The weights of the flood variables were calculated using N-DEMATEL model through evaluating criteria based on their expected significances. The integration of GIS-environment with N-DEMATEL technique provides more flexibility to assess the causative agents of flooding.

We identified flood influencing factors and by using these factors in multi-criteria analysis we developed a flood susceptibility map of the study area. Regarding our flood influencing factors, the elevation factor was within the range from 17 m to 879 m . The slope factor was within the range from 0° to 66.6° .The topographic wetness index was within the range from 2.6648 to 26.3782. The aspect factor was grouped into ten classes : [Flat (-1) , North (0-22.5)

Doi: https://doi.org/10.54216/FPA.120105
Received: January 17, 2023 Revised: April 25, 2023 Accepted: June 09, 2023

, Northeast (22.5-67.5) , East (67.5-112.5) , Southeast (112.5-157.5) , South (157.5-202.5) , Southwest (202.5-247.5) , West (247.5-292.5), Northwest (292.5-337.5) and North (337.5-360)) . The hydrological parameters for the study area including flow direction, flow Accumulation, watersheds and drainage density can be seen in Figure 7 , Figure 8 , Figure 13 and Figure 16 . The soil factor was grouped into four classes: (Gravels and gravelly sand soil , Water , stony soils and Nile alluvium) . The LULC factor was grouped into four classes: (Stony_Area , Bare_Soil, Vegetation and Urban) . The precipitation factor was within the range from 2.8 mm to 16.3327 mm. The curvature factor was within the range from -14.92 to 12.7. The distance from streams factor was within the range from 0 m to 2696.4 m. By using the N- DEMATEL multi-criteria analysis method, the weight of each factor calculated and obtained the following results: 0.067037378 for Population Density, 0.066978636 for Total Population, 0.066754041 for Precipitation, 0.066496641 for Distance From Stream, 0.066489133 for Elevation, 0.066384715 for Drainage Density, 0.066328707 for Soil, 0.06637841 for (LULC), 0.066355817 for (Slope), 0.066417786 for Flow Direction, 0.066444645 for Flow Accumulation, 0.066809228 for TWI, 0.066892234 for Curvature, 0.06695252 for Aspect and 0.06728011 for Watershed. Flood hazard map and was generated using the following equation:

$$FHM = \Sigma (C1Wj1 + C2Wj2 + C3Wj3 + CnWjn),$$

Where, Wj is the weight of each factor; n is the number of factors, $C1$, $C2, C3$, and Cn are the respective factors. In our study, five classes were identified: very high, high, moderate, low, and very low.

The resulting hazard map shows that Manfalut , Asyut and Al-Qusiyyah are the most vulnerable to flooding, while Al-Ghanayim, Asyut1, Asyut2 and New Asyut are the least vulnerable to flooding. as seen in Figure .20, Figure .21 and Figure .21.

Our results reveal that ‘very high’ susceptibility category reflects approximately 5 %. Whilst the ‘high’ susceptibility class reflects approximately 12% and the ‘moderate’ susceptibility category covers approximately 26%. Furthermore, the ‘low’ susceptibility category reflects approximately 35% and the ‘very low’ susceptibility class reflects approximately 22% of our study area.

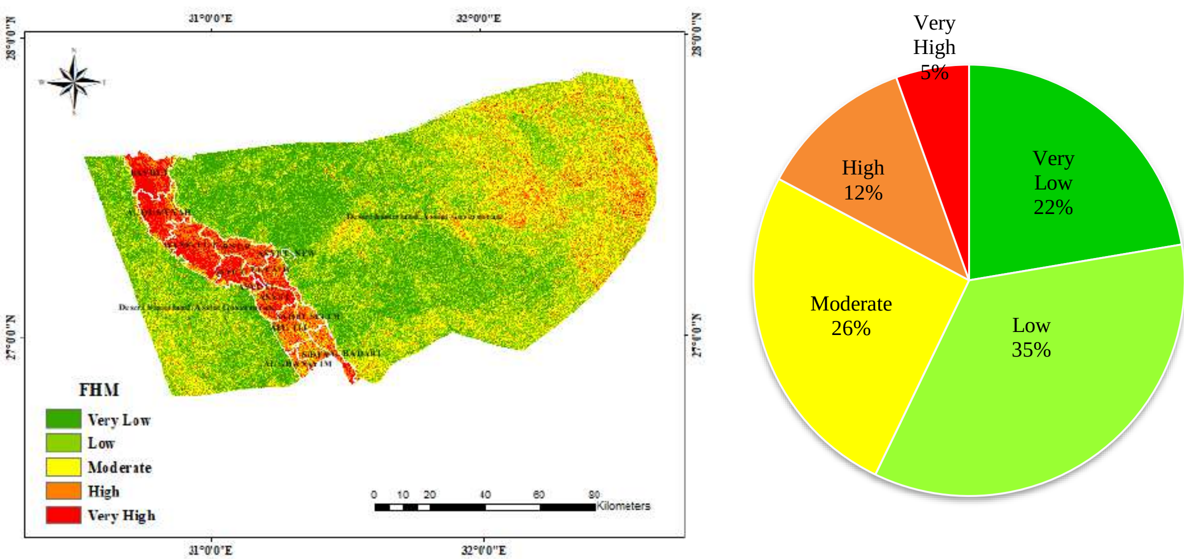

.

Figure 20: Susceptibility map

Doi: https://doi.org/10.54216/FPA.120105
Received: January 17, 2023 Revised: April 25, 2023 Accepted: June 09, 2023

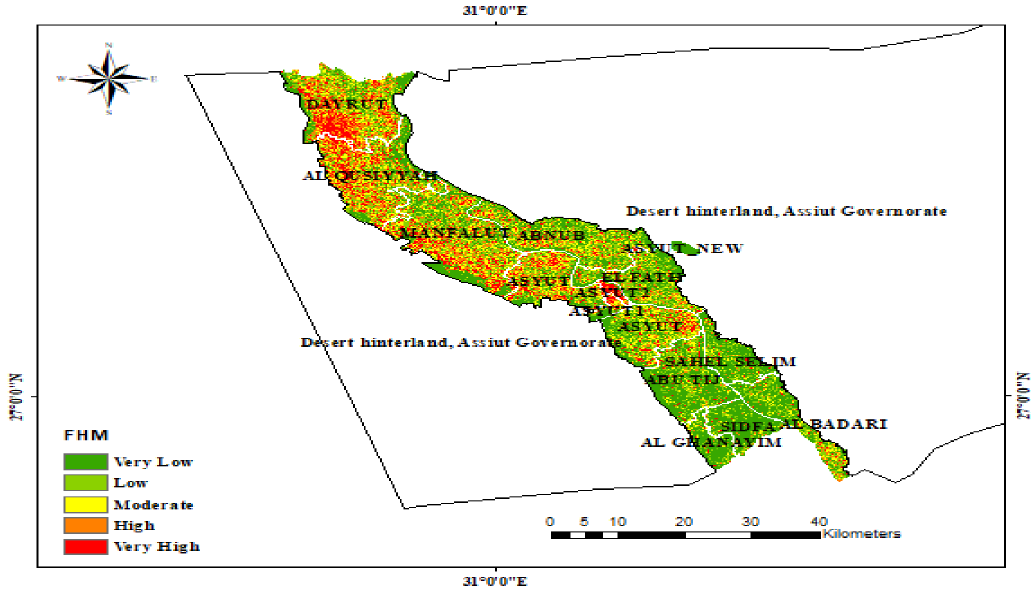

Figure 21: Flood hazard map

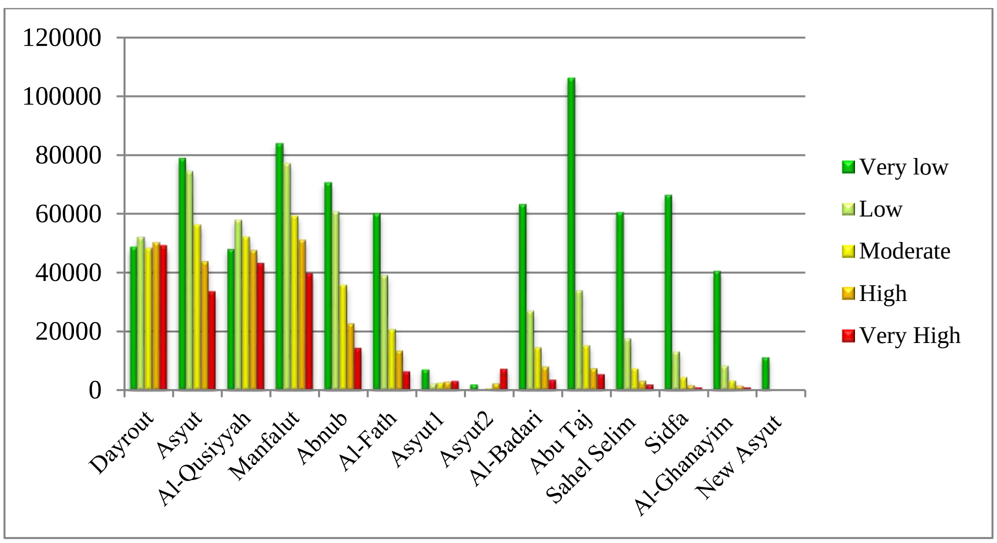

Figure 22: Vulnerability Percentages in Asyut's urban districts

7. Concluding Remarks

Flood susceptibility map provides valuable data for decision-makers and the planners dealing with flood hazards and susceptibility. Flood susceptibility map provides residents with information about probable damage and how to prevent potential disasters. Our study area is in Upper Egypt in the Asyut governorate. To analyze the influence of flash floods on study area, fifteen influencing factors such as elevation, slope, topographic wetness index, distance from the stream, flow accumulation, aspect, flow direction, soil , land cover , watershed , curvature , drainage density , total population , population density and precipitation were determined. The weight of each factor calculated by using the N-DEMATEL multi criteria analysis method and obtained the following results: 0.067037378 for Population Density, 0.066978636 for Total Population, 0.066754041 for Precipitation, 0.066496641 for Distance From Stream, 0.066489133 for Elevation, 0.066384715 for Drainage Density, 0.066328707 for Soil, 0.06637841 for (LULC), 0.066355817 for (Slope), 0.066417786 for Flow Direction, 0.066444645 for Flow Accumulation, 0.066809228 for TWI, 0.066892234 for Curvature, 0.06695252 for Aspect and 0.06728011 for Watershed. Our

Doi: https://doi.org/10.54216/FPA.120105
Received: January 17, 2023 Revised: April 25, 2023 Accepted: June 09, 2023

results reveal that 'very high' susceptibility category reflects approximately 5 %. whilst the 'high' susceptibility class reflects approximately 12% and the 'moderate' susceptibility category covers approximately 26%. Furthermore, the 'low' susceptibility category reflects approximately 35% and the 'very low' susceptibility class reflects approximately 22% of our study area. From our study, we concluded that the integration of remotely sensed data and geographical information system (GIS) with neutrosophic DEMATEL is a valuable and an appropriate tool to assess flash flood susceptibility.

In the future, we will analyze the influence of flash floods on various study areas using various neutrosophic MCDM techniques and geographical information system.

Limitation of Proposed Research: More involvements from more companies will make our research better.

Competing Interests

The authors announce that there is no discrepancy of interest concerning the publication of this research.

Acknowledgments

The authors would like to thank the anonymous referees for their insightful and constructive comments and suggestions.

References

[1] Elmoustafa, A.M., Mohamed, M.M., 2013. Flash flood risk assessment using morphological parameters in Sinai Peninsula. Open J. Mod. Hydrol. 3, 122–129. https://doi.org/10.4236/ojmh.2013.33016.

[2] Mohamed, S. A., & El-Raey, M. E. (2020). Vulnerability assessment for flash floods using GIS spatial modeling and remotely sensed data in El-Arish City, North Sinai, Egypt. Natural Hazards, 102(2), 707-728.

[3] Mohamed, S. A. (2021). Development of a GIS-based alert system to mitigate flash flood impacts in Asyut governorate, Egypt. Natural hazards, 108(3), 2739-2763.

[4] Veijalainen, N., Jakkila, J., Olsson, T., Backman, L., Vehviläinen, B., & Kaurola, J. (2017). Impacts of climate change on extreme floods in Finland–studies using bias corrected Regional Climate Model data. Hydrology and Earth System Sciences Discussions, 1-28.

[5] Maghsood, F. F., Moradi, H., Massah Bavani, A. R., Panahi, M., Berndtsson, R., & Hashemi, H. (2019). Climate change impact on flood frequency and source area in northern Iran under CMIP5 scenarios. Water, 11(2), 273.

[6] Ahmadi, S., Amjadi, H., Chapi, K., Soodmand Afshar, R., & Ebrahimi, B. (2022). Fuzzy flash flood risk and vulnerability assessment for the city of Sanandaj, Kurdistan Province, Iran. Natural Hazards, 1-23.

[7] Abu El-Magd, S. A., Maged, A., & Farhat, H. I. (2022). Hybrid-based Bayesian algorithm and hydrologic indices for flash flood vulnerability assessment in coastal regions: machine learning, risk prediction, and environmental impact. Environmental Science and Pollution Research, 1-12.

[8] Khosravi, K., Pourghasemi, H. R., Chapi, K., & Bahri, M. (2016). Flash flood susceptibility analysis and its mapping using different bivariate models in Iran: a comparison between Shannon's entropy, statistical index, and weighting factor models. Environmental monitoring and assessment, 188(12), 1-21

[9] El-Magd, S. A. A., Amer, R. A., & Embaby, A. (2020). Multi-criteria decision-making for the analysis of flash floods: a case study of Awlad Toq-Sherq, Southeast Sohag, Egypt. Journal of African Earth Sciences, 162, 103709.

[10] Monsef, H. A. E. (2018). A mitigation strategy for reducing flood risk to highways in arid regions: a case study of the El-Quseir–Qena highway in Egypt. Journal of Flood Risk Management, 11, S158-S172.

[11] Abuzied, S. M., & Mansour, B. M. (2019). Geospatial hazard modeling for the delineation of flash flood-prone zones in Wadi Dahab basin, Egypt. Journal of Hydroinformatics, 21(1), 180-206.

[12] Abdel-Fattah, M., Saber, M., Kantoush, S. A., Khalil, M. F., Sumi, T., & Sefelnasr, A. M. (2017). A hydrological and geomorphometric approach to understanding the generation of wadi flash floods. Water, 9(7), 553.

[13] Hagos, Y. G., Andualem, T. G., Yibeltal, M., & Mengie, M. A. (2022). Flood hazard assessment and mapping using GIS integrated with multi-criteria decision analysis in upper Awash River basin, Ethiopia. Applied Water Science, 12(7), 1-18.

[14] Wu, J., Chen, X., & Lu, J. (2022). Assessment of long and short-term flood risk using the multi-criteria analysis model with the AHP-Entropy method in Poyang Lake basin. International Journal of Disaster Risk Reduction, 75, 102968.

Doi: https://doi.org/10.54216/FPA.120105
Received: January 17, 2023 Revised: April 25, 2023 Accepted: June 09, 2023

[15] Kadaverugu, A., Kadaverugu, R., Chintala, N. R., & Gorthi, K. V. (2022). Flood vulnerability assessment of urban micro-watersheds using multi-criteria decision making and InVEST model: a case of Hyderabad City, India. Modeling Earth Systems and Environment, 8(3), 3447-3459.
[16] Loi, D. T., Tuan, P. A., & Manh, N. V. (2022). Detecting Flash Flood Susceptible Areas Using a Multicriteria Decision-Making Model: A Case Study of Thai Nguyen Province, Vietnam. In Global Changes and Sustainable Development in Asian Emerging Market Economies Vol. 2 (pp. 451-464). Springer, Cham.
[17] Idrees, M. O., Yusuf, A., Mokhtar, E. S., & Yao, K. (2022). Urban flood susceptibility mapping in Ilorin, Nigeria, using GIS and multi-criteria decision analysis. Modeling Earth Systems and Environment, 8(4), 5779-5791.
[18] Dahri, N., Yousfi, R., Bouamrane, A., Abida, H., Pham, Q. B., & Derdous, O. (2022). Comparison of analytic network process and artificial neural network models for flash flood susceptibility assessment. Journal of African Earth Sciences, 193, 104576.
[19] Lyu, H. M., Shen, S. L., Yin, Z. Y., & Zhou, A. (2022). Anp-Gis-Based Approach for Risk Assessment of Typhoon-Induced Floods in Coastal Cities. Available at SSRN 4164017.
[20] Gabus, A., & Fontela, E. J. B. G. R. C. (1972). World problems, an invitation to further thought within the framework of DEMATEL. Battelle Geneva Research Center, Geneva, Switzerland, 1(8).
[21] Si, S. L., You, X. Y., Liu, H. C., & Zhang, P. (2018). DEMATEL technique: A systematic review of the state-of-the-art literature on methodologies and applications. Mathematical Problems in Engineering, 2018, 1-33.
[22] Skilodimou, H. D., Bathrellos, G. D., Chousianitis, K., Youssef, A. M., & Pradhan, B. (2019). Multi-hazard assessment modeling via multi-criteria analysis and GIS: a case study. Environmental Earth Sciences, 78(2), 1-21.
[23] Rincón, D., Khan, U. T., & Armenakis, C. (2018). Flood risk mapping using GIS and multi-criteria analysis: A greater Toronto area case study. Geosciences, 8(8), 275.
[24] Youssef, A. M., & Hegab, M. A. (2019). Flood-hazard assessment modeling using multicriteria analysis and GIS: a case study—Ras Gharib area, Egypt. In Spatial modeling in GIS and R for earth and environmental sciences (pp. 229-257). Elsevier.
[25] Ganová, L. (2011). Integrating multicriteria analysis with geographical information system for evaluation flood vulnerable areas. International Multidisciplinary Scientific GeoConference: SGEM, 2, 433.
[26] Tang, Z., Zhang, H., Yi, S., & Xiao, Y. (2018). Assessment of flood susceptible areas using spatially explicit, probabilistic multi-criteria decision analysis. Journal of Hydrology, 558, 144-158.
[27] Heba R. Abdelhady,Mahmoud M. Ismail, Cardiovascular Diseases Forecasting using Machine Learning Models, International Journal of Advances in Applied Computational Intelligence, Vol. 1 , No. 2 , (2022) : 56-62 (Doi : https://doi.org/10.54216/IJAACI.010204)
[28] Sayed, Y. A., El-Desoky, M. A., Gameh, M. A., & Faragallah, M. A. (2016). Land capability of some soils representing western limestone Plateau at Assiut. Assiut J. Agric. Sci, 47(3), 120-141.
[29] Rose Aljanada,Ghadeer W. Abukhalil,Aseel M. Alfaisal,Raghad M. Alfaisal, Adoption of Google Glass technology: PLS-SEM and machine learning analysis, International Journal of Advances in Applied Computational Intelligence, Vol. 1 , No. 1 , (2022) : 08-22 (Doi : https://doi.org/10.54216/IJAACI.010101)
[30] Talukdar, S., Ghose, B., Salam, R., Mahato, S., Pham, Q. B., Linh, N. T. T., ... & Avand, M. (2020). Flood susceptibility modeling in Teesta River basin, Bangladesh using novel ensembles of bagging algorithms. Stochastic Environmental Research and Risk Assessment, 34(12), 2277-2300.
[31] Abdel-Basset, M., Mohamed, M., Hussien, A. N., & Sangaiah, A. K. (2018). A novel group decision-making model based on triangular neutrosophic numbers. Soft Computing, 22(20), 6629-6643.
[32] Wang, H., Zhang, Y. Q., & Sunderraman, R. (2005, July). Truth-value based interval neutrosophic sets. In 2005 IEEE International Conference on Granular Computing (Vol. 1, pp. 274-277). IEEE.
[33] Ahmed Sleem,Ibrahim Elhenawy, An Interval Valued Neutrosophic Sets Integrated with the AHP MCDM Methodology to Assess the Station of 5G Network, Neutrosophic and Information Fusion, Vol. 1 , No. 1 , (2023) : 34-40 (Doi : https://doi.org/10.54216/NIF.010104)
[34] Mona Mohamed,Nissreen El Saber, Prioritization Thermochemical Materials based on Neutrosophic sets Hybrid MULTIMOORA Ranker Method, Neutrosophic and Information Fusion, Vol. 2 , No. 1 , (2023) : 08-22 (Doi : https://doi.org/10.54216/NIF.020101)
[35] Sušinskas, S., Zavadskas, E. K., & Turskis, Z. (2011). Multiple criteria assessment of pile-columns alternatives. The Baltic Journal of Road and Bridge Engineering, 6(3), 145-152.

Doi: https://doi.org/10.54216/FPA.120105
Received: January 17, 2023 Revised: April 25, 2023 Accepted: June 09, 2023

Appendix A : Normalize the direct-relation decision matrix

Normalize the direct-relation decision matrix T lower

	C1	C2	C3	C4	C5	C6	C7	C8	C9	C10	C11	C12	C13	C14	C15
C1	0.036	0.054	0.054	0.057	0.057	0.057	0.068	0.064	0.057	0.068	0.068	0.068	0.068	0.071	0.071
C2	0.050	0.036	0.054	0.057	0.057	0.057	0.068	0.064	0.057	0.068	0.068	0.068	0.068	0.071	0.071
C3	0.050	0.050	0.036	0.064	0.057	0.054	0.057	0.057	0.054	0.068	0.064	0.068	0.068	0.071	0.071
C4	0.046	0.046	0.043	0.036	0.054	0.057	0.054	0.064	0.057	0.068	0.068	0.068	0.068	0.071	0.071
C5	0.046	0.046	0.046	0.050	0.036	0.057	0.054	0.057	0.057	0.064	0.064	0.068	0.064	0.064	0.071
C6	0.046	0.046	0.050	0.046	0.046	0.036	0.057	0.064	0.057	0.068	0.068	0.068	0.068	0.071	0.071
C7	0.039	0.039	0.046	0.050	0.050	0.046	0.036	0.054	0.054	0.057	0.054	0.064	0.068	0.064	0.064
C8	0.043	0.043	0.046	0.043	0.046	0.043	0.050	0.036	0.054	0.057	0.057	0.064	0.068	0.064	0.064
C9	0.046	0.046	0.050	0.046	0.046	0.046	0.050	0.050	0.036	0.054	0.054	0.057	0.057	0.064	0.064
C10	0.039	0.039	0.039	0.039	0.043	0.039	0.046	0.046	0.050	0.036	0.054	0.057	0.057	0.064	0.064
C11	0.039	0.039	0.043	0.039	0.043	0.039	0.050	0.046	0.050	0.050	0.036	0.057	0.057	0.064	0.064
C12	0.039	0.039	0.039	0.039	0.039	0.039	0.043	0.043	0.046	0.046	0.046	0.036	0.054	0.057	0.057
C13	0.039	0.039	0.039	0.039	0.043	0.039	0.039	0.039	0.046	0.046	0.046	0.050	0.036	0.057	0.057
C14	0.036	0.036	0.036	0.036	0.043	0.036	0.043	0.043	0.043	0.043	0.043	0.046	0.046	0.036	0.064
C15	0.036	0.036	0.036	0.036	0.036	0.036	0.043	0.043	0.043	0.043	0.043	0.046	0.046	0.043	0.036

Normalize the direct-relation decision matrix T upper

	C1	C2	C3	C4	C5	C6	C7	C8	C9	C10	C11	C12	C13	C14	C15
C1	0.036	0.061	0.061	0.064	0.064	0.064	0.071	0.068	0.064	0.071	0.071	0.071	0.071	0.071	0.071
C2	0.057	0.036	0.061	0.064	0.064	0.064	0.071	0.068	0.064	0.071	0.071	0.071	0.071	0.071	0.071
C3	0.057	0.057	0.036	0.068	0.064	0.061	0.064	0.064	0.061	0.071	0.068	0.071	0.071	0.071	0.071
C4	0.054	0.054	0.050	0.036	0.061	0.064	0.061	0.068	0.064	0.071	0.071	0.071	0.071	0.071	0.071
C5	0.054	0.054	0.054	0.057	0.036	0.064	0.061	0.064	0.064	0.068	0.068	0.071	0.068	0.068	0.071

Doi: https://doi.org/10.54216/FPA.120105
Received: January 17, 2023 Revised: April 25, 2023 Accepted: June 09, 2023

C6	**0.054**	**0.054**	**0.057**	**0.054**	**0.054**	**0.036**	**0.064**	**0.068**	**0.064**	**0.071**	**0.071**	**0.071**	**0.071**	**0.071**	**0.071**
C7	**0.046**	**0.046**	**0.054**	**0.057**	**0.057**	**0.054**	**0.036**	**0.061**	**0.061**	**0.064**	**0.061**	**0.068**	**0.071**	**0.068**	**0.068**
C8	**0.050**	**0.050**	**0.054**	**0.050**	**0.054**	**0.050**	**0.057**	**0.036**	**0.061**	**0.064**	**0.064**	**0.068**	**0.071**	**0.068**	**0.068**
C9	**0.054**	**0.054**	**0.057**	**0.054**	**0.054**	**0.054**	**0.057**	**0.057**	**0.036**	**0.061**	**0.061**	**0.064**	**0.064**	**0.068**	**0.068**
C10	**0.046**	**0.046**	**0.046**	**0.046**	**0.050**	**0.046**	**0.054**	**0.054**	**0.057**	**0.036**	**0.061**	**0.064**	**0.064**	**0.068**	**0.068**
C11	**0.046**	**0.046**	**0.050**	**0.046**	**0.050**	**0.046**	**0.057**	**0.054**	**0.057**	**0.057**	**0.036**	**0.064**	**0.064**	**0.068**	**0.068**
C12	**0.046**	**0.046**	**0.046**	**0.046**	**0.046**	**0.046**	**0.050**	**0.050**	**0.054**	**0.054**	**0.054**	**0.036**	**0.061**	**0.064**	**0.064**
C13	**0.046**	**0.046**	**0.046**	**0.046**	**0.050**	**0.046**	**0.046**	**0.046**	**0.054**	**0.054**	**0.054**	**0.057**	**0.036**	**0.064**	**0.064**
C14	**0.043**	**0.043**	**0.043**	**0.043**	**0.050**	**0.043**	**0.050**	**0.050**	**0.050**	**0.050**	**0.050**	**0.054**	**0.054**	**0.036**	**0.068**
C15	**0.043**	**0.043**	**0.043**	**0.043**	**0.043**	**0.043**	**0.050**	**0.050**	**0.050**	**0.050**	**0.050**	**0.054**	**0.054**	**0.050**	**0.036**

Normalize the direct-relation decision matrix I lower

	C1	**C2**	**C3**	**C4**	**C5**	**C6**	**C7**	**C8**	**C9**	**C10**	**C11**	**C12**	**C13**	**C14**	**C15**
C1	**0.085**	**0.017**	**0.017**	**0.008**	**0.008**	**0.008**	**0.000**	**0.000**	**0.008**	**0.000**	**0.000**	**0.000**	**0.000**	**0.000**	**0.000**
C2	**0.025**	**0.085**	**0.017**	**0.008**	**0.008**	**0.008**	**0.000**	**0.000**	**0.008**	**0.000**	**0.000**	**0.000**	**0.000**	**0.000**	**0.000**
C3	**0.025**	**0.025**	**0.085**	**0.000**	**0.008**	**0.017**	**0.008**	**0.008**	**0.017**	**0.000**	**0.000**	**0.000**	**0.000**	**0.000**	**0.000**
C4	**0.034**	**0.034**	**0.042**	**0.085**	**0.017**	**0.008**	**0.017**	**0.000**	**0.008**	**0.000**	**0.000**	**0.000**	**0.000**	**0.000**	**0.000**
C5	**0.034**	**0.034**	**0.034**	**0.025**	**0.085**	**0.008**	**0.017**	**0.008**	**0.008**	**0.000**	**0.000**	**0.000**	**0.000**	**0.000**	**0.000**
C6	**0.034**	**0.034**	**0.025**	**0.034**	**0.034**	**0.085**	**0.008**	**0.000**	**0.008**	**0.000**	**0.000**	**0.000**	**0.000**	**0.000**	**0.000**
C7	**0.051**	**0.051**	**0.034**	**0.025**	**0.025**	**0.034**	**0.085**	**0.017**	**0.017**	**0.008**	**0.017**	**0.000**	**0.000**	**0.000**	**0.000**
C8	**0.042**	**0.042**	**0.034**	**0.042**	**0.034**	**0.042**	**0.025**	**0.085**	**0.017**	**0.008**	**0.008**	**0.000**	**0.000**	**0.000**	**0.000**
C9	**0.034**	**0.034**	**0.025**	**0.034**	**0.034**	**0.034**	**0.025**	**0.025**	**0.085**	**0.017**	**0.017**	**0.008**	**0.008**	**0.000**	**0.000**
C10	**0.051**	**0.051**	**0.051**	**0.051**	**0.042**	**0.051**	**0.034**	**0.034**	**0.025**	**0.085**	**0.017**	**0.008**	**0.008**	**0.000**	**0.000**
C11	**0.051**	**0.051**	**0.042**	**0.051**	**0.042**	**0.051**	**0.025**	**0.034**	**0.025**	**0.025**	**0.085**	**0.008**	**0.008**	**0.000**	**0.000**
C12	**0.051**	**0.051**	**0.051**	**0.051**	**0.051**	**0.051**	**0.042**	**0.042**	**0.034**	**0.034**	**0.034**	**0.085**	**0.017**	**0.008**	**0.008**
C13	**0.051**	**0.051**	**0.051**	**0.051**	**0.042**	**0.051**	**0.051**	**0.051**	**0.034**	**0.034**	**0.034**	**0.025**	**0.085**	**0.008**	**0.008**

Doi: https://doi.org/10.54216/FPA.120105
Received: January 17, 2023 Revised: April 25, 2023 Accepted: June 09, 2023

C14	0.059	0.059	0.059	0.059	0.042	0.059	0.042	0.042	0.042	0.042	0.042	0.034	0.034	0.085	0.000
C15	0.059	0.059	0.059	0.059	0.059	0.059	0.042	0.042	0.042	0.042	0.042	0.034	0.034	0.042	0.085

Normalize the direct-relation decision matrix I upper

	C1	C2	C3	C4	C5	C6	C7	C8	C9	C10	C11	C12	C13	C14	C15
C1	0.085	0.034	0.034	0.017	0.017	0.017	0.000	0.008	0.017	0.000	0.000	0.000	0.000	0.000	0.000
C2	0.042	0.085	0.034	0.017	0.017	0.017	0.000	0.008	0.017	0.000	0.000	0.000	0.000	0.000	0.000
C3	0.042	0.042	0.085	0.008	0.017	0.034	0.017	0.017	0.034	0.000	0.008	0.000	0.000	0.000	0.000
C4	0.051	0.051	0.059	0.085	0.034	0.017	0.034	0.008	0.017	0.000	0.000	0.000	0.000	0.000	0.000
C5	0.051	0.051	0.051	0.042	0.085	0.017	0.034	0.017	0.017	0.008	0.008	0.000	0.008	0.008	0.000
C6	0.051	0.051	0.042	0.051	0.051	0.085	0.017	0.008	0.017	0.000	0.000	0.000	0.000	0.000	0.000
C7	0.068	0.068	0.051	0.042	0.042	0.051	0.085	0.034	0.034	0.017	0.034	0.008	0.000	0.008	0.008
C8	0.059	0.059	0.051	0.059	0.051	0.059	0.042	0.085	0.034	0.017	0.017	0.008	0.000	0.008	0.008
C9	0.051	0.051	0.042	0.051	0.051	0.051	0.042	0.042	0.085	0.034	0.034	0.017	0.017	0.008	0.008
C10	0.068	0.068	0.068	0.068	0.059	0.068	0.051	0.051	0.042	0.085	0.034	0.017	0.017	0.008	0.008
C11	0.068	0.068	0.059	0.068	0.059	0.068	0.042	0.051	0.042	0.042	0.085	0.017	0.017	0.008	0.008
C12	0.068	0.068	0.068	0.068	0.068	0.068	0.059	0.059	0.051	0.051	0.051	0.085	0.034	0.017	0.017
C13	0.068	0.068	0.068	0.068	0.059	0.068	0.068	0.068	0.051	0.051	0.051	0.042	0.085	0.017	0.017
C14	0.076	0.076	0.076	0.076	0.059	0.076	0.059	0.059	0.059	0.059	0.059	0.051	0.051	0.085	0.008
C15	0.076	0.076	0.076	0.076	0.076	0.076	0.059	0.059	0.059	0.059	0.059	0.051	0.051	0.059	0.085

Normalize the direct-relation decision matrix F lower

	C1	C2	C3	C4	C5	C6	C7	C8	C9	C10	C11	C12	C13	C14	C15
C1	0.071	0.021	0.021	0.014	0.014	0.014	0.000	0.007	0.014	0.000	0.000	0.000	0.000	0.000	0.000
C2	0.029	0.071	0.021	0.014	0.014	0.014	0.000	0.007	0.014	0.000	0.000	0.000	0.000	0.000	0.000

Doi: https://doi.org/10.54216/FPA.120105
Received: January 17, 2023 Revised: April 25, 2023 Accepted: June 09, 2023

C3	0.029	0.029	0.071	0.007	0.014	0.021	0.014	0.014	0.021	0.000	0.007	0.000	0.000	0.000	0.000
C4	0.036	0.036	0.043	0.071	0.021	0.014	0.021	0.007	0.014	0.000	0.000	0.000	0.000	0.000	0.000
C5	0.036	0.036	0.036	0.029	0.071	0.014	0.021	0.014	0.014	0.007	0.007	0.000	0.007	0.007	0.000
C6	0.036	0.036	0.029	0.036	0.036	0.071	0.014	0.007	0.014	0.000	0.000	0.000	0.000	0.000	0.000
C7	0.050	0.050	0.036	0.029	0.029	0.036	0.071	0.021	0.021	0.014	0.021	0.007	0.000	0.007	0.007
C8	0.043	0.043	0.036	0.043	0.036	0.043	0.029	0.071	0.021	0.014	0.014	0.007	0.000	0.007	0.007
C9	0.036	0.036	0.029	0.036	0.036	0.036	0.029	0.029	0.071	0.021	0.021	0.014	0.014	0.007	0.007
C10	0.050	0.050	0.050	0.050	0.043	0.050	0.036	0.036	0.029	0.071	0.021	0.014	0.014	0.007	0.007
C11	0.050	0.050	0.043	0.050	0.043	0.050	0.029	0.036	0.029	0.029	0.071	0.014	0.014	0.007	0.007
C12	0.050	0.050	0.050	0.050	0.050	0.050	0.043	0.043	0.036	0.036	0.036	0.071	0.021	0.014	0.014
C13	0.050	0.050	0.050	0.050	0.043	0.050	0.050	0.050	0.036	0.036	0.036	0.029	0.071	0.014	0.014
C14	0.057	0.057	0.057	0.057	0.043	0.057	0.043	0.043	0.043	0.043	0.043	0.036	0.036	0.071	0.007
C15	0.057	0.057	0.057	0.057	0.057	0.057	0.043	0.043	0.043	0.043	0.043	0.036	0.036	0.043	0.071

Normalize the direct-relation decision matrix F upper

	C1	C2	C3	C4	C5	C6	C7	C8	C9	C10	C11	C12	C13	C14	C15
C1	0.071	0.036	0.036	0.029	0.029	0.029	0.014	0.021	0.029	0.014	0.014	0.014	0.014	0.000	0.000
C2	0.043	0.071	0.036	0.029	0.029	0.029	0.014	0.021	0.029	0.014	0.014	0.014	0.014	0.000	0.000
C3	0.043	0.043	0.071	0.021	0.029	0.036	0.029	0.029	0.036	0.014	0.021	0.014	0.014	0.000	0.000
C4	0.050	0.050	0.057	0.071	0.036	0.029	0.036	0.021	0.029	0.014	0.014	0.014	0.014	0.000	0.000
C5	0.050	0.050	0.050	0.043	0.071	0.029	0.036	0.029	0.029	0.021	0.021	0.014	0.021	0.021	0.000
C6	0.050	0.050	0.043	0.050	0.050	0.071	0.029	0.021	0.029	0.014	0.014	0.014	0.014	0.000	0.000
C7	0.064	0.064	0.050	0.043	0.043	0.050	0.071	0.036	0.036	0.029	0.036	0.021	0.014	0.021	0.021
C8	0.057	0.057	0.050	0.057	0.050	0.057	0.043	0.071	0.036	0.029	0.029	0.021	0.014	0.021	0.021
C9	0.050	0.050	0.043	0.050	0.050	0.050	0.043	0.043	0.071	0.036	0.036	0.029	0.029	0.021	0.021
C10	0.064	0.064	0.064	0.064	0.057	0.064	0.050	0.050	0.043	0.071	0.036	0.029	0.029	0.021	0.021
C11	0.064	0.064	0.057	0.064	0.057	0.064	0.043	0.050	0.043	0.043	0.071	0.029	0.029	0.021	0.021

Doi: https://doi.org/10.54216/FPA.120105
Received: January 17, 2023 Revised: April 25, 2023 Accepted: June 09, 2023

C12	**0.064**	**0.064**	**0.064**	**0.064**	**0.064**	**0.064**	**0.057**	**0.057**	**0.050**	**0.050**	**0.050**	**0.071**	**0.036**	**0.029**	**0.029**
C13	**0.064**	**0.064**	**0.064**	**0.064**	**0.057**	**0.064**	**0.064**	**0.064**	**0.050**	**0.050**	**0.050**	**0.043**	**0.071**	**0.029**	**0.029**
C14	**0.071**	**0.071**	**0.071**	**0.071**	**0.057**	**0.071**	**0.057**	**0.057**	**0.057**	**0.057**	**0.057**	**0.050**	**0.050**	**0.071**	**0.021**
C15	**0.071**	**0.071**	**0.071**	**0.071**	**0.071**	**0.071**	**0.057**	**0.057**	**0.057**	**0.057**	**0.057**	**0.050**	**0.050**	**0.057**	**0.071**

Doi: https://doi.org/10.54216/FPA.120105
Received: January 17, 2023 Revised: April 25, 2023 Accepted: June 09, 2023